



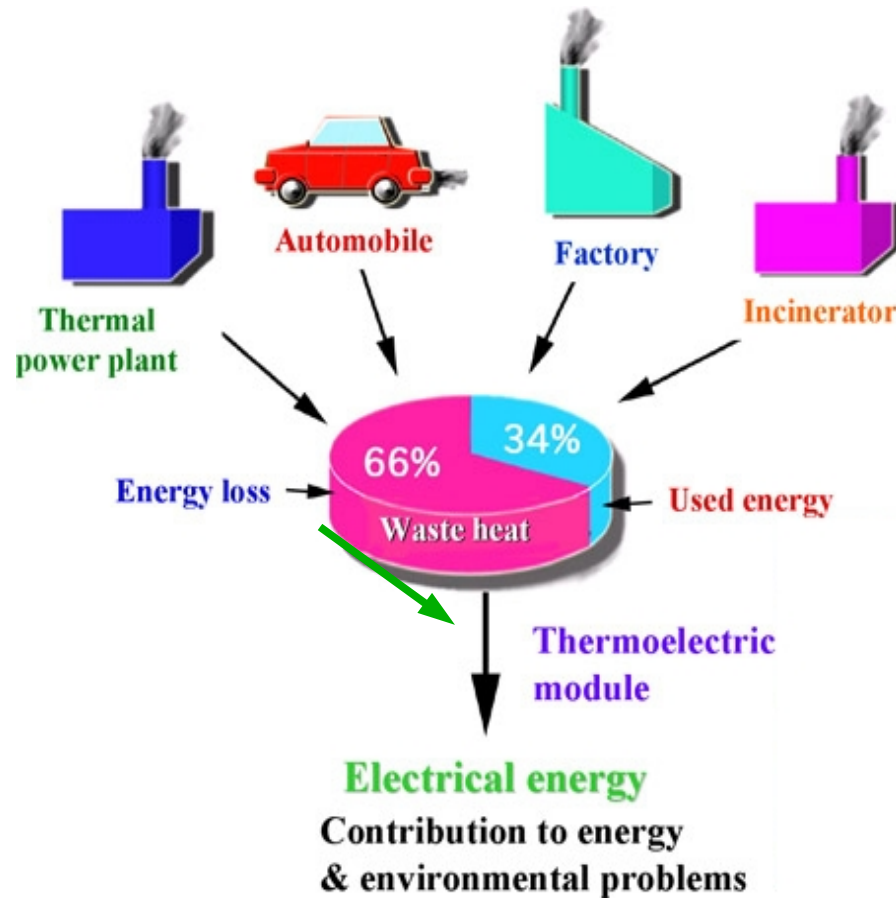
Thermoelectric materials

Raphaël Hermann

Jülich Centre for Neutron Science and Peter Grünberg Institut, Forschungszentrum Jülich GmbH, Germany

Université de Liège, Faculté des Sciences, Belgium

Efficient Thermal Management



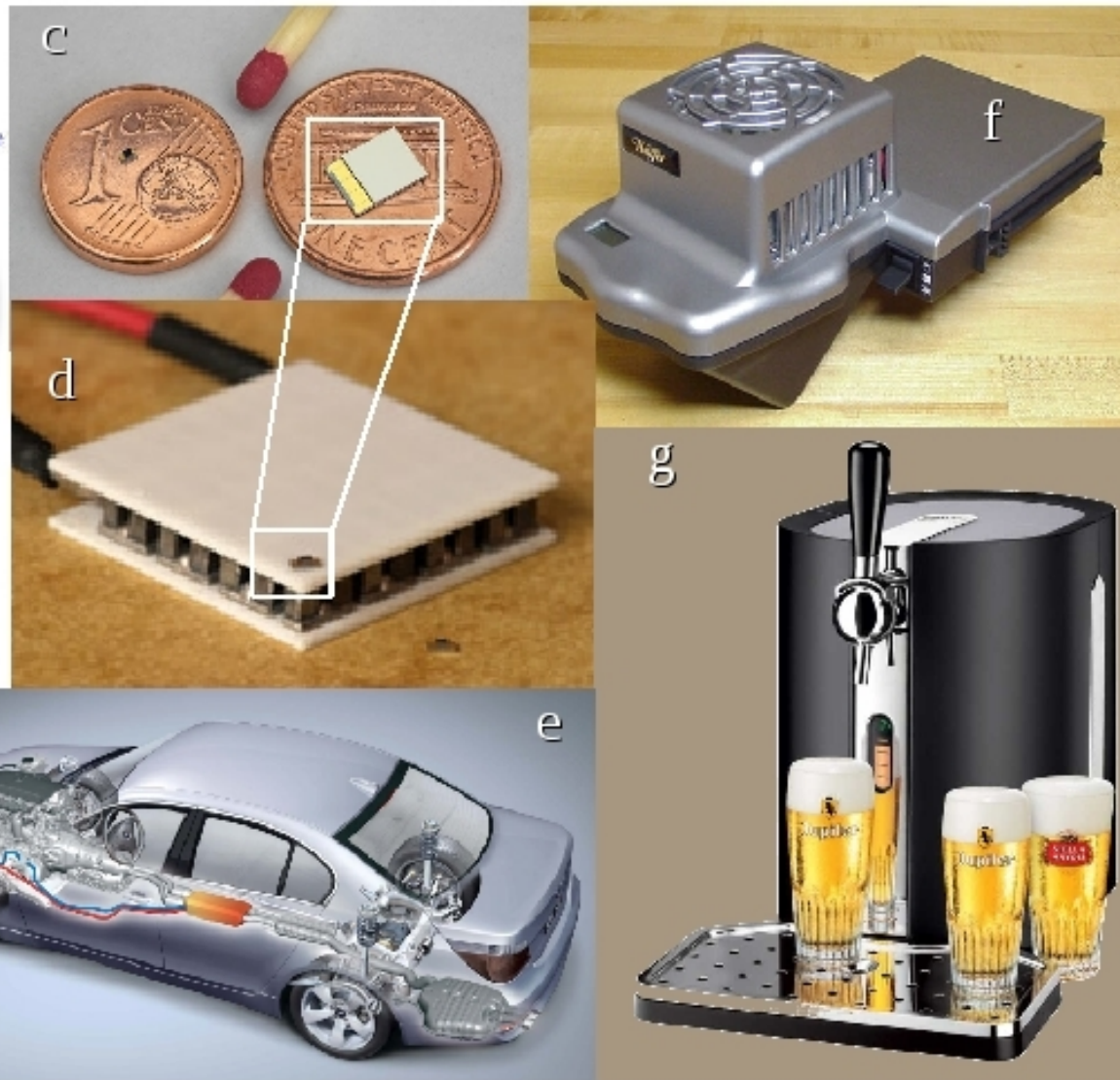
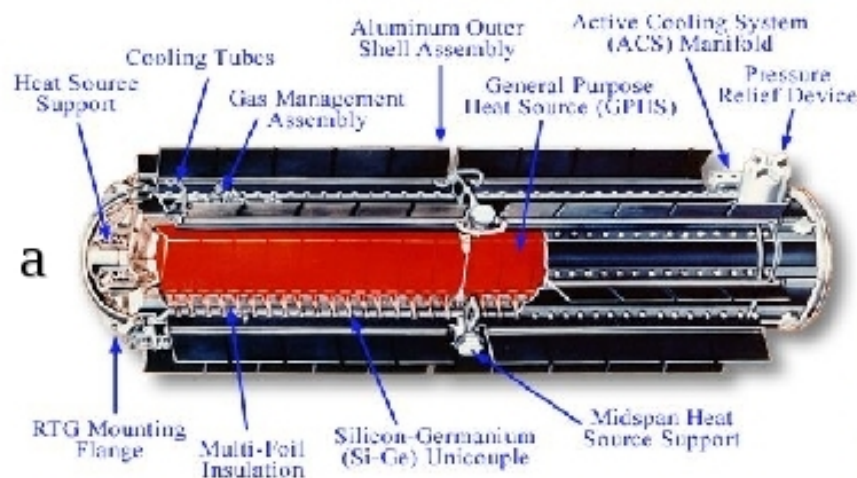
Efficiency of waste heat: 0%

Efficiency of thermoelectric converters: >7-8%

~10% fuel economy for the automotive industry.

Applications

GPHS-RTG

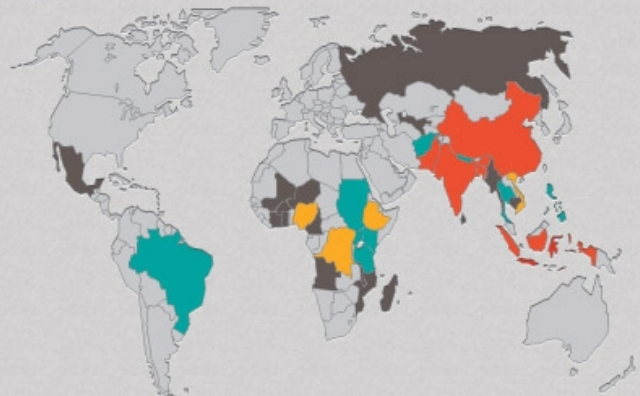


Sources: a,b WikiMedia (NASA, JPL); c,d MicroPelt; e BMW; f,g: Commercials

Worldwide number of people cooking on open fires

3 billion people worldwide cook on open fires

1.3 billion of these lack access to electricity

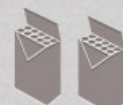


● Over 100 million ● Over 50 million ● Over 20 million ● Over 10 million

1 billion metric tons of CO₂ from cooking fires are released into the atmosphere each year

2 million people die each year from indoor smoke from inefficient cooking fires (more than twice as many as malaria)

Many hours spent per week collecting fuel.



Health effects from indoor smoke are equivalent to smoking *two packs of cigarettes daily*.



CO₂e emissions per year (metric tons)

Average car	5.1
Three-stone fire	5.3

Cost to reduce CO₂e emission by 1 metric ton



Average amount of income spent on energy

20-30% of income

Average amount the world's poor spend on fuel alone

4% of income

Average amount Americans spend on energy

Annual savings by an average family in India using the HomeStove

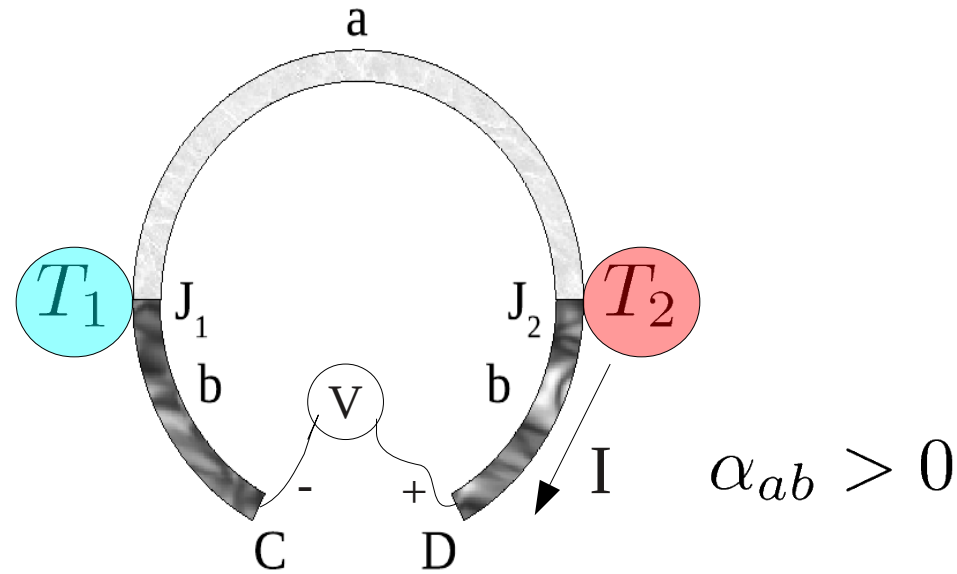
\$72

- Electricity savings (cell phone charging, switching from kerosene to LED lighting)
- Fuel savings from more efficient burning

Introduction: A brief history – Seebeck effect



T. Seebeck
(1770-1831)



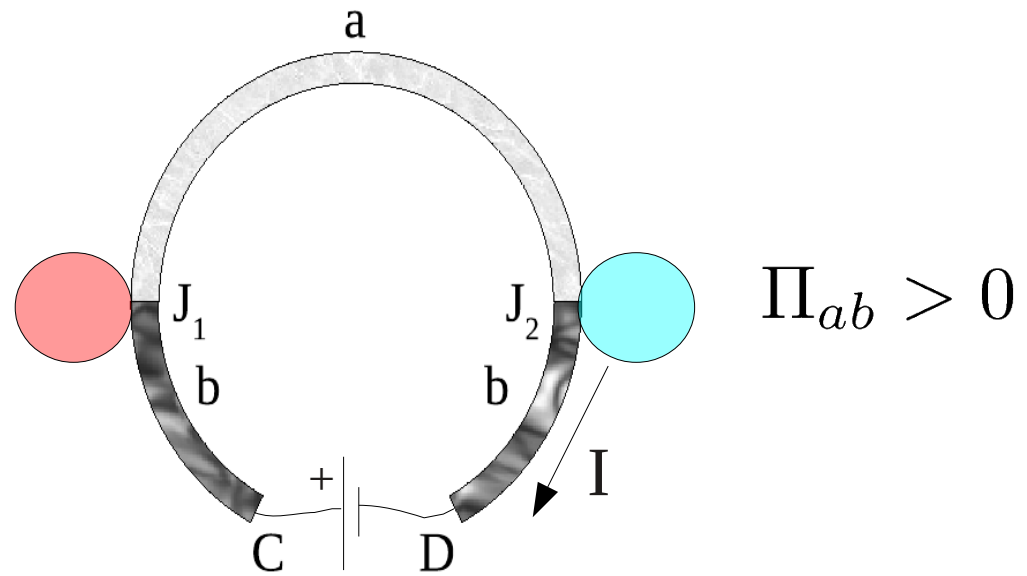
$$V = (\alpha_b - \alpha_a)(T_2 - T_1) = \alpha_{ab}\Delta T$$

- Depends on the temperature difference and not on the specific geometry!
- Original mistake by Seebeck: „Magnetic polarization ... by temperature difference“
- Clarified by Oersted: thermo-electric effect

Introduction: A brief history – Peltier effect



J.-C. Peltier
(1785-1845)



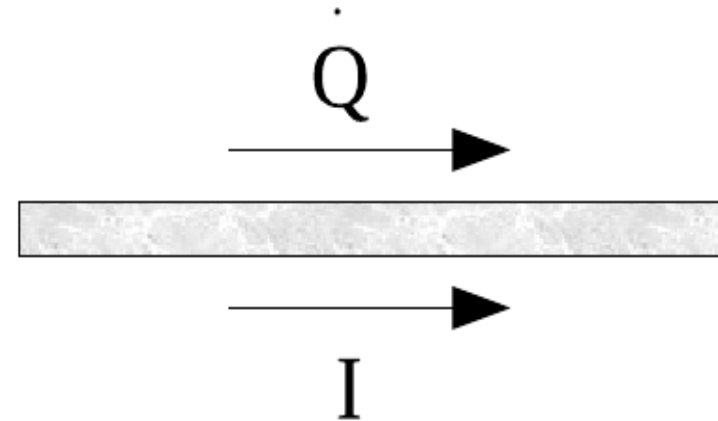
$$\dot{Q} = (\Pi_b - \Pi_a) \cdot I = \Pi_{ab} \cdot I$$

- Heating or cooling of the junctions is reversible with the current sign

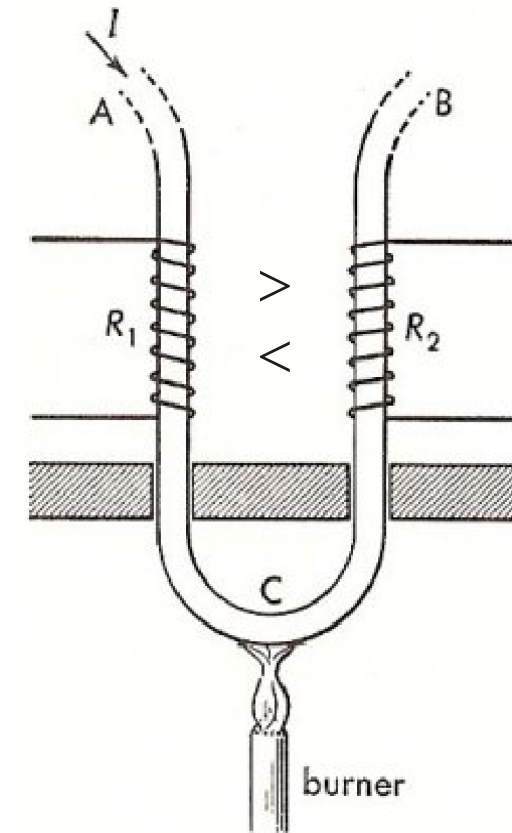
Introduction: A brief history – Thomson effect



W. Thomson
(1824-1907)



$$\dot{Q} = RI^2 - \mu_T I \Delta T$$



Duckworth, Electricity and magnetism

- Heating of R_1 and cooling of R_2 or conversely depending on the sign of I and μ
- Predicted effect, then verified experimentally
- $\mu < 0$ in Bi, Fe, Pt, ... and > 0 in Sb, Cu, Ag, μ is $f(T)$ and can reverse sign.

Introduction: Unifying thermoelectricity

Kelvin relations



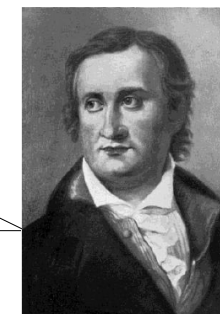
J.-C. Peltier
 (1785-1845)



W. Thomson
 Lord Kelvin
 (1824-1907)

$$\mu_T = T \frac{d\alpha}{dT}$$

$$\rightarrow \Pi = \alpha T \leftarrow$$



T. Seebeck
 (1770-1831)

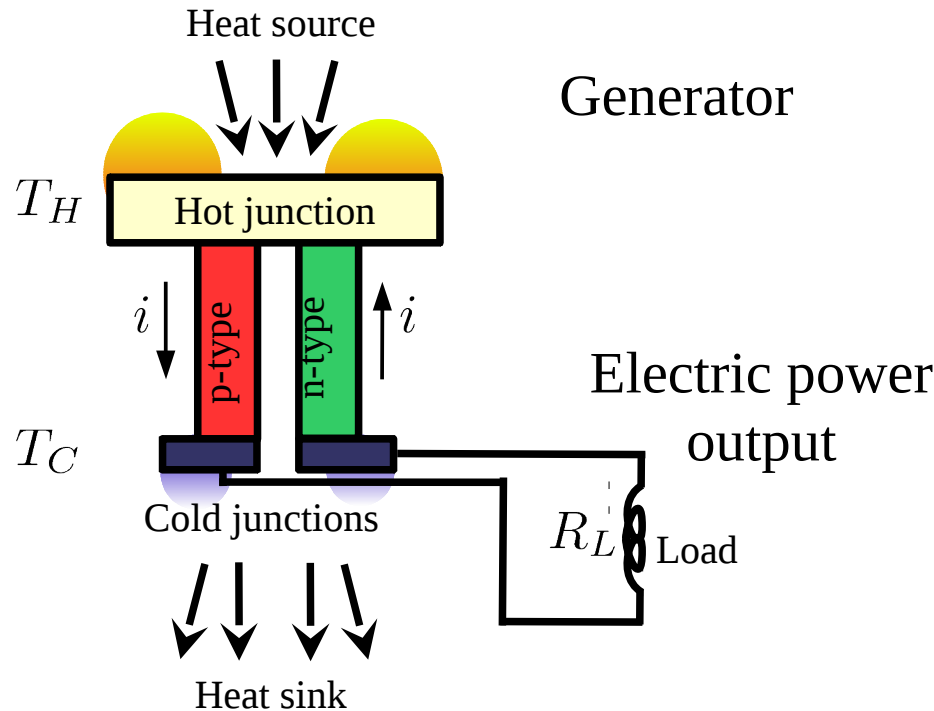
Consequences of
 non-equilibrium thermodynamics

- For a superconductor, $\alpha = 0$ (e.g. Pb for $T < 7$ K)
- The Peltier and Seebeck coefficients can be defined for a single material

$$\alpha = \int d\alpha = \int \mu(T) \cdot dT/T$$

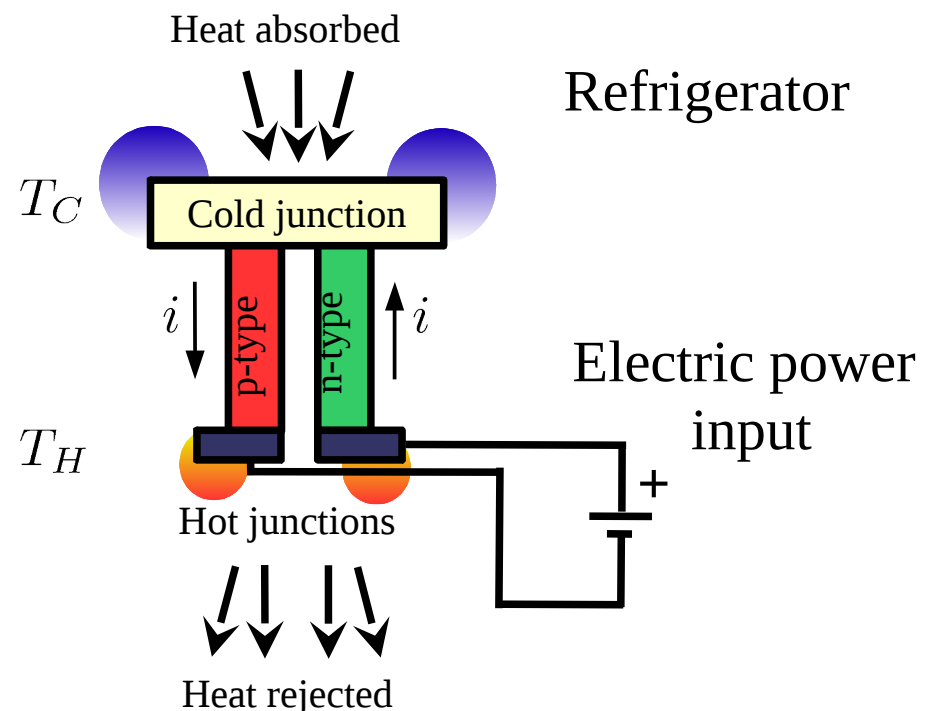
Thermoelectric conversion

Seebeck effect



Generator

Peltier effect

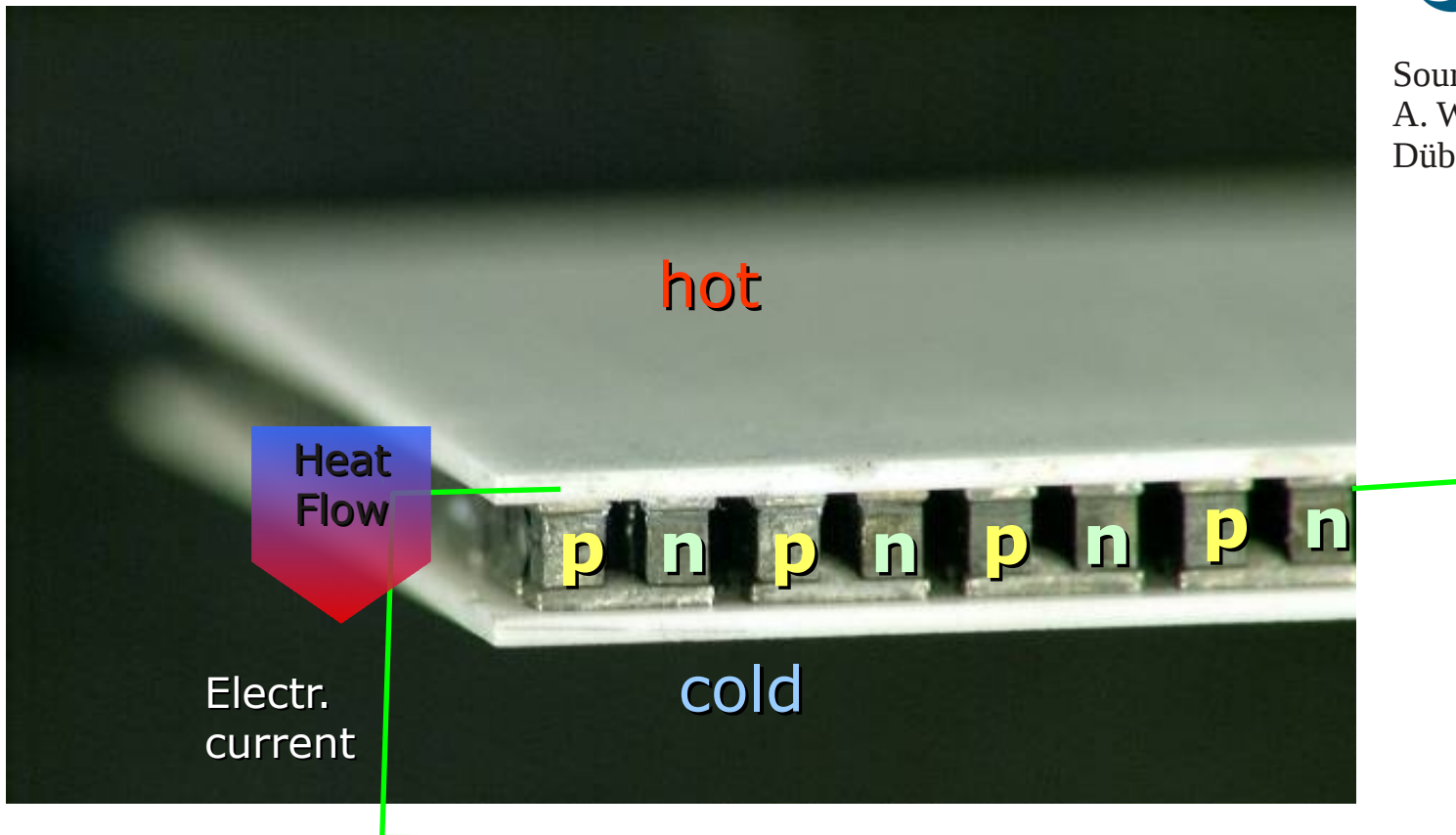


Refrigerator

- No moving parts
- Direct conversion: clean and silent
- High power density: small size
- No scale merit, small ΔT

Thermoelectric conversion

Source:
A. Weidenkaff, EMPA
Dübendorf



- Device: junctions thermally in parallel, electrically in series
- Efficiency?
- Upper limit: Carnot efficiency

$$\eta < \eta_C = \frac{T_H - T_C}{T_C}$$

$$\eta = \eta_C \frac{\sqrt{1 + Z_{ab}T_{av}} - 1}{\sqrt{1 + Z_{ab}T_{av}} + T_C/T_H}$$

Thermoelectricity: finding a compromise

$$ZT = \frac{\alpha^2 \sigma}{\kappa} T$$

Electric conductivity

$$\sigma = ne\mu$$

Thermopower

$$\alpha = \frac{8\pi^2 k_B^2}{3eh^2} m^* T \left(\frac{\pi}{3n}\right)^{2/3}$$

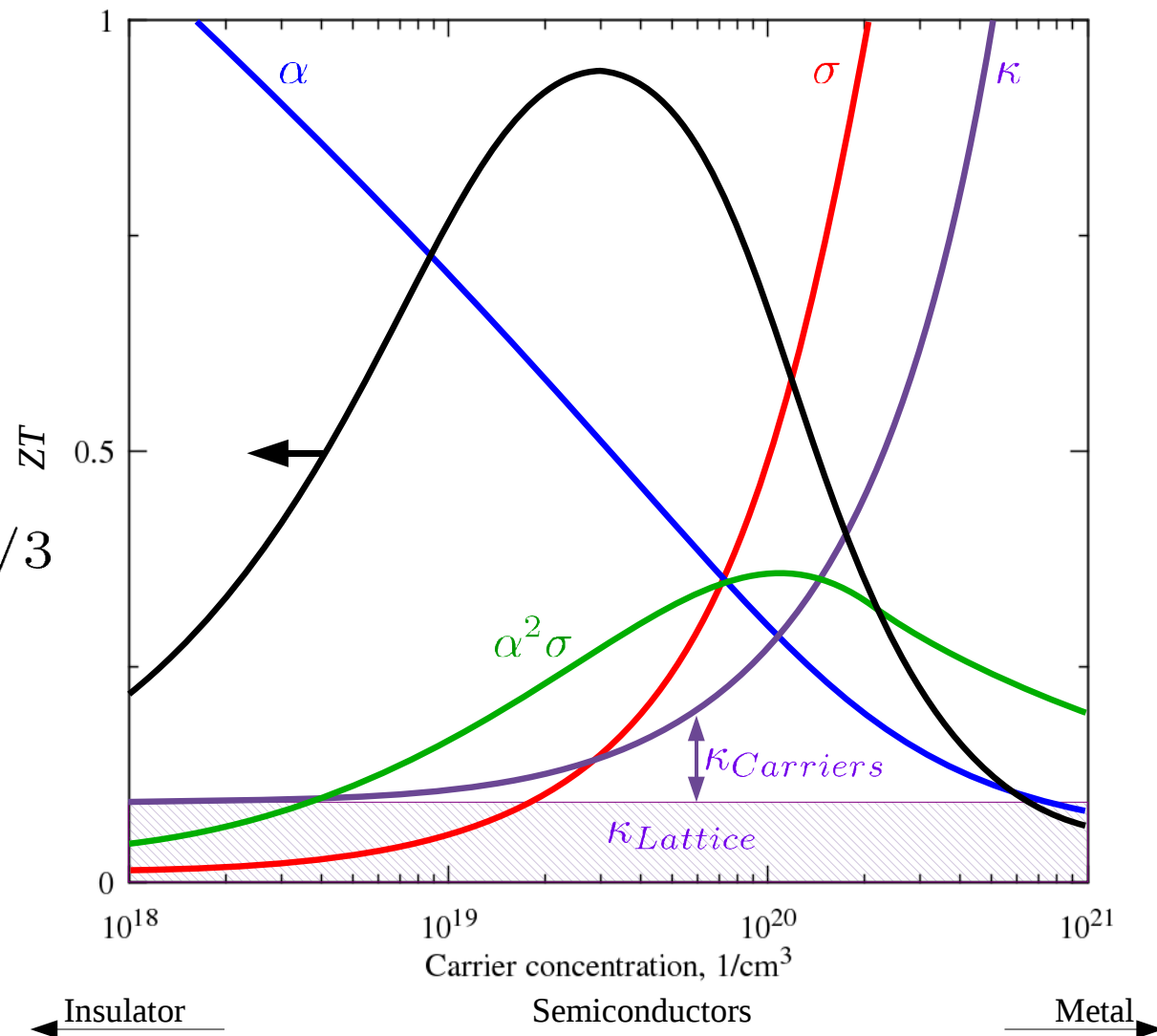
Charge carrier thermal conductivity

$$\kappa_e / \sigma \approx L \cdot T$$

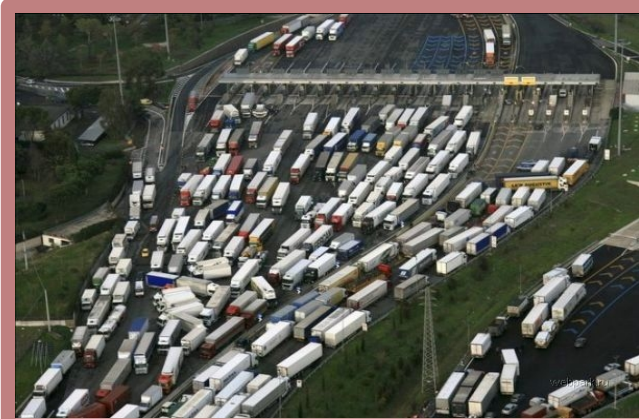
Total thermal conductivity

$$\kappa = \kappa_e + \boxed{\kappa_l}$$

Debye model: $\kappa_l \approx \frac{1}{3} c_v v_s \lambda_{ph} = \frac{1}{3} c_v v_s^2 \tau_{ph}$



Thermal conductivity



$$\kappa_L = 1/V \sum_{i,k} v_{i,x}^2(k) \tau_i(k) C_i(k)$$

Low mean phonon velocity

- guest host interaction
- soft materials

Low phonon mean free path

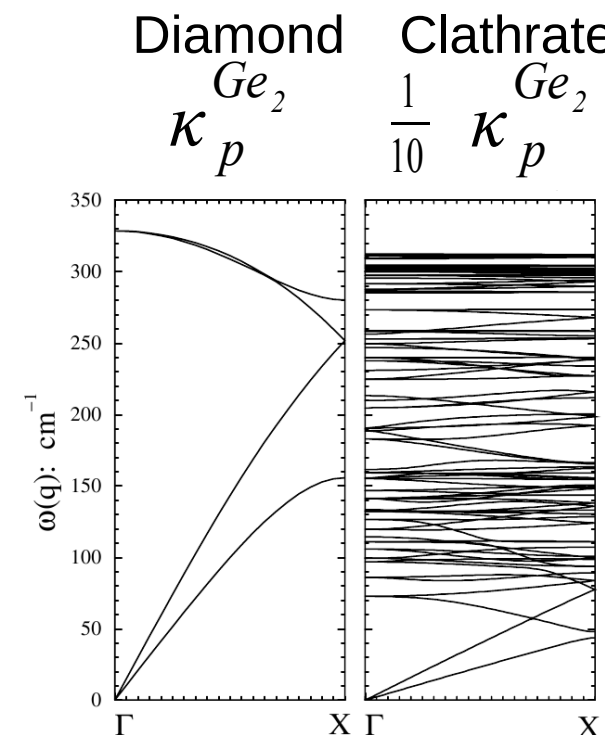
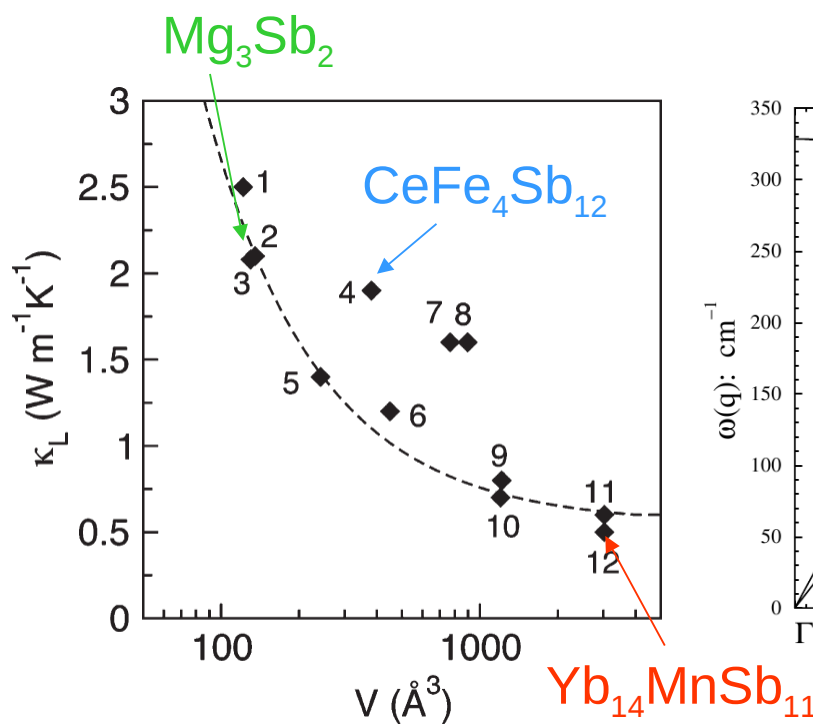
- guest and host interaction
- nanostructuring
- anharmonicity

Low 'specific heat' contribution

- large unit cell

Effective Heat Capacity

$$\kappa_p = \frac{1}{3} C_V v_s \lambda$$



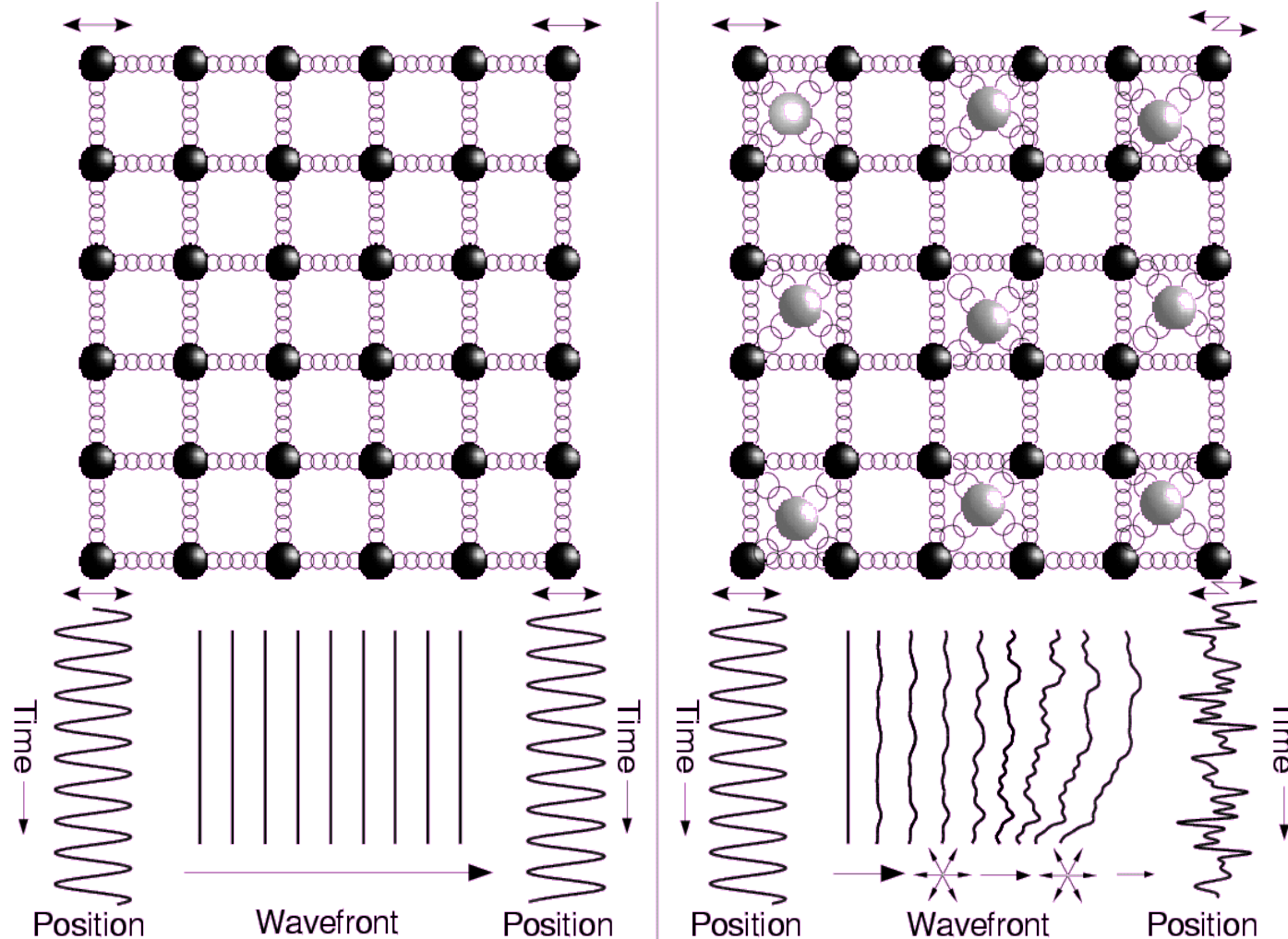
Large unit cell → small ratio of the number of acoustic to optical modes
 → small contribution of the heat capacity to the thermal conductivity

$$C_V \rightarrow C_V^{eff}$$

Phonon mean free path

$$\kappa_p = \frac{1}{3} C_V v_s \lambda$$

→ interaction of guest and cage atom



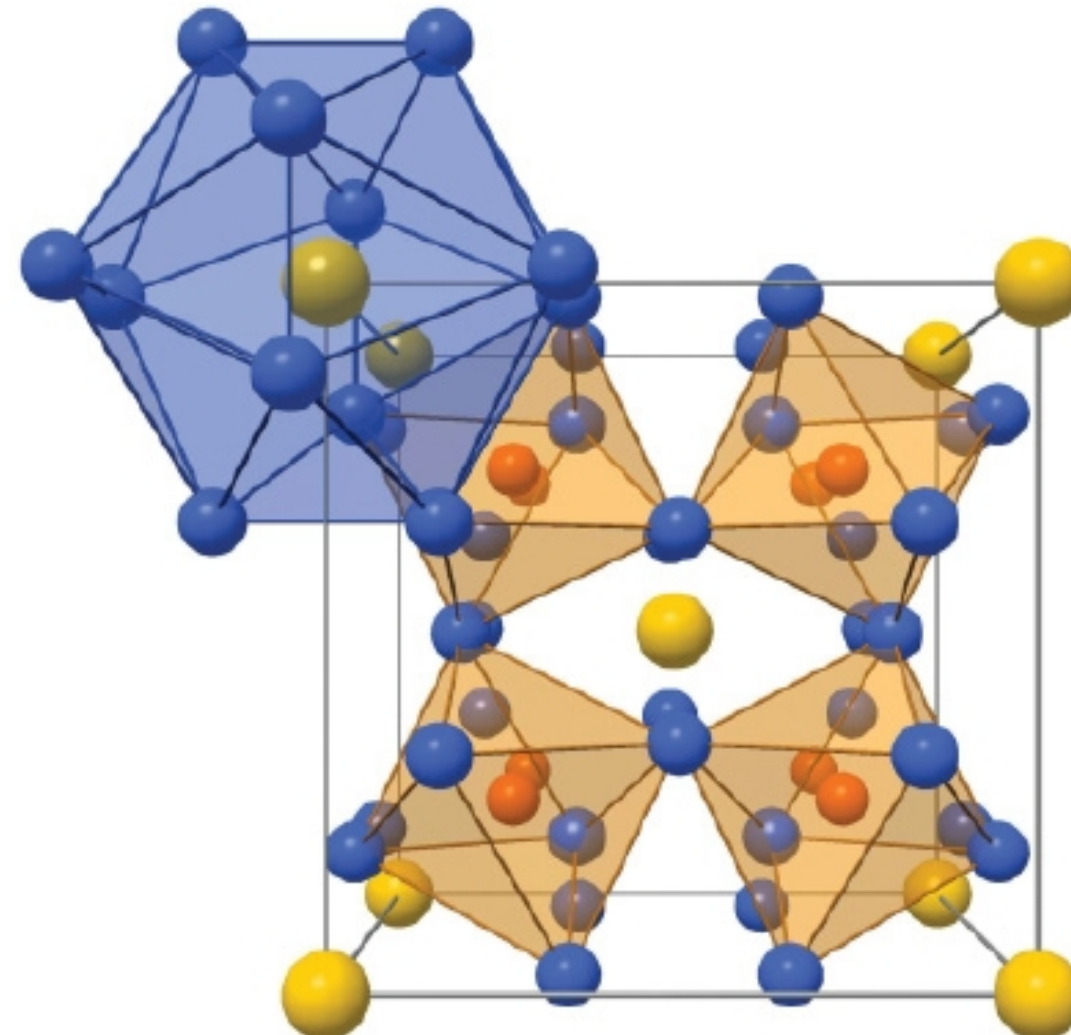
YbFe₄Sb₁₂

PHYSICAL REVIEW B **84**, 184306 (2011)

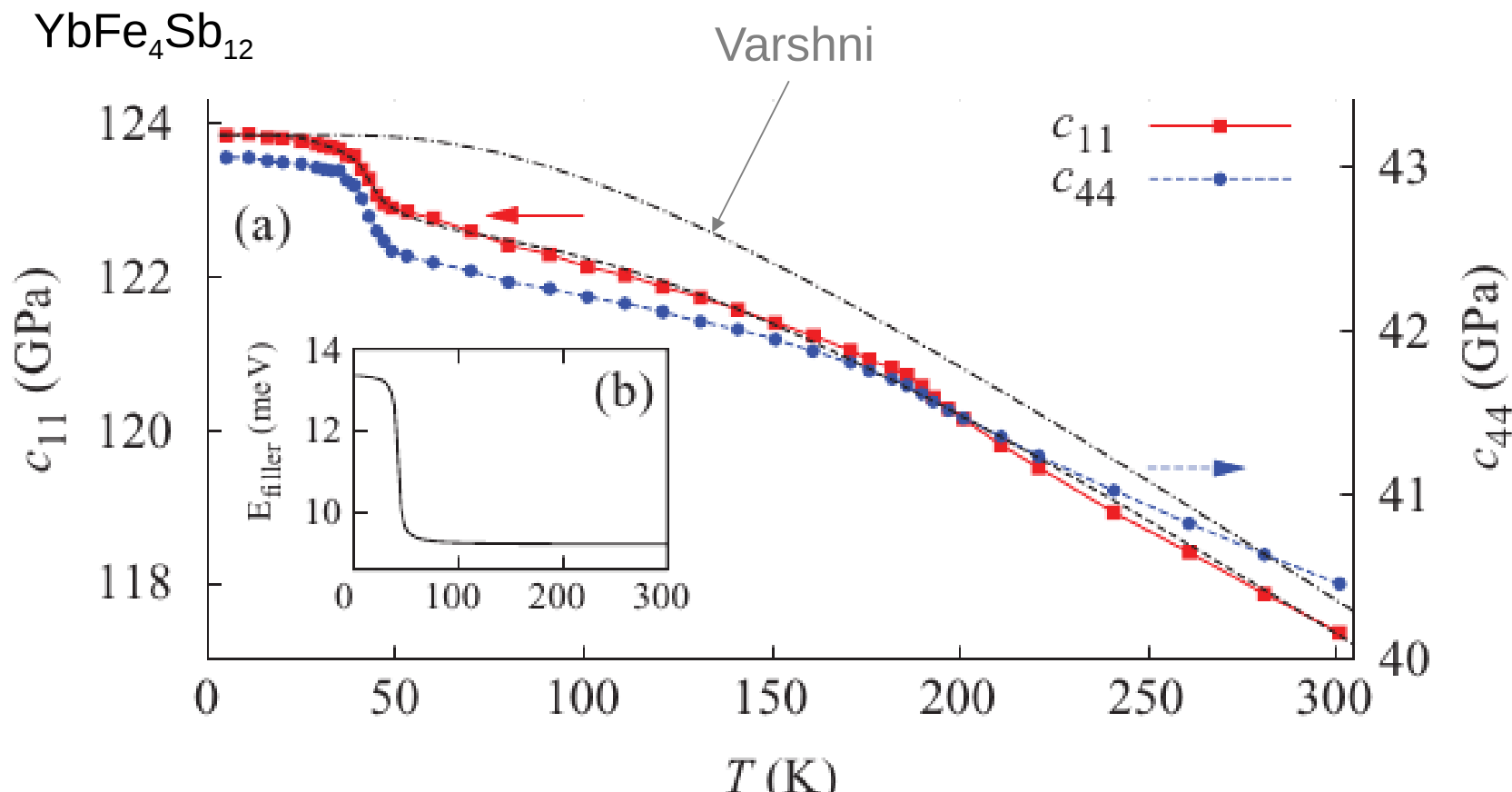


Lattice dynamics and anomalous softening in the YbFe₄Sb₁₂ skutterudite

A. Möchel,^{1,2} I. Sergueev,³ H.-C. Wille,⁴ J. Voigt,¹ M. Prager,^{1,*} M. B. Stone,⁵ B. C. Sales,⁶ Z. Guguchia,⁷ A. Shengelaya,⁷ V. Keppens,⁸ and R. P. Hermann^{1,2,†}



Resonant ultrasound spectroscopy



Possible explanations:

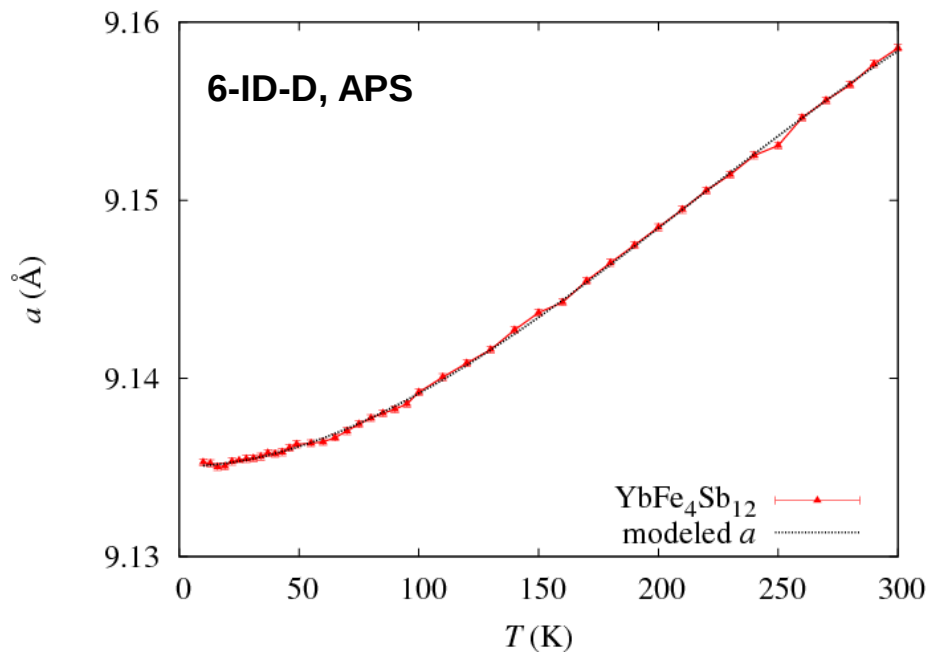
- structural phase transition
- magnetic phase transition
- shift of the guest mode energy
- Yb valence change

V. Keppens, University of Tennessee

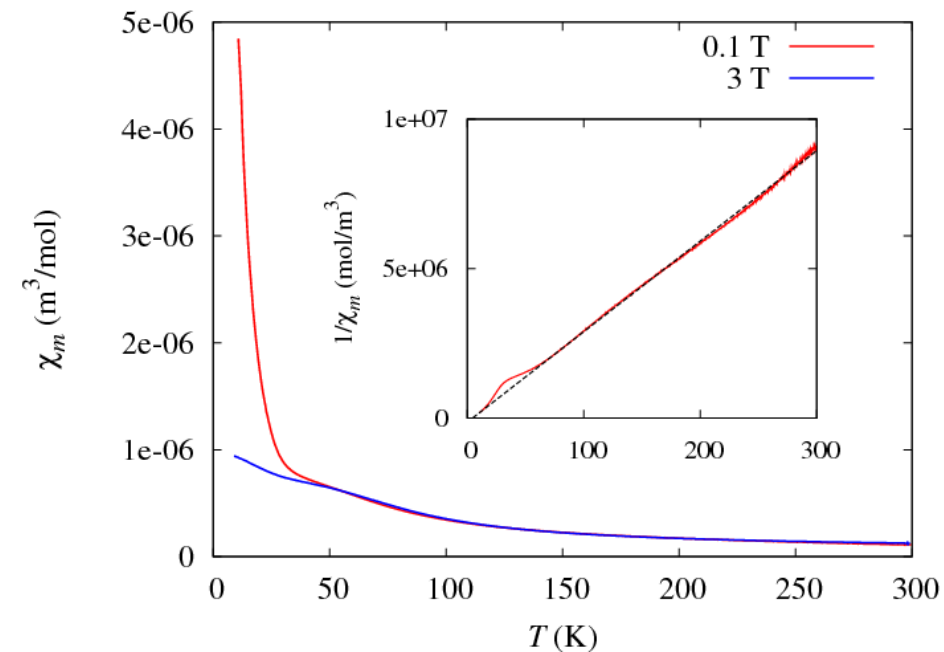
Phase transition



Diffraction



Magnetometry (VSM, PPMS)

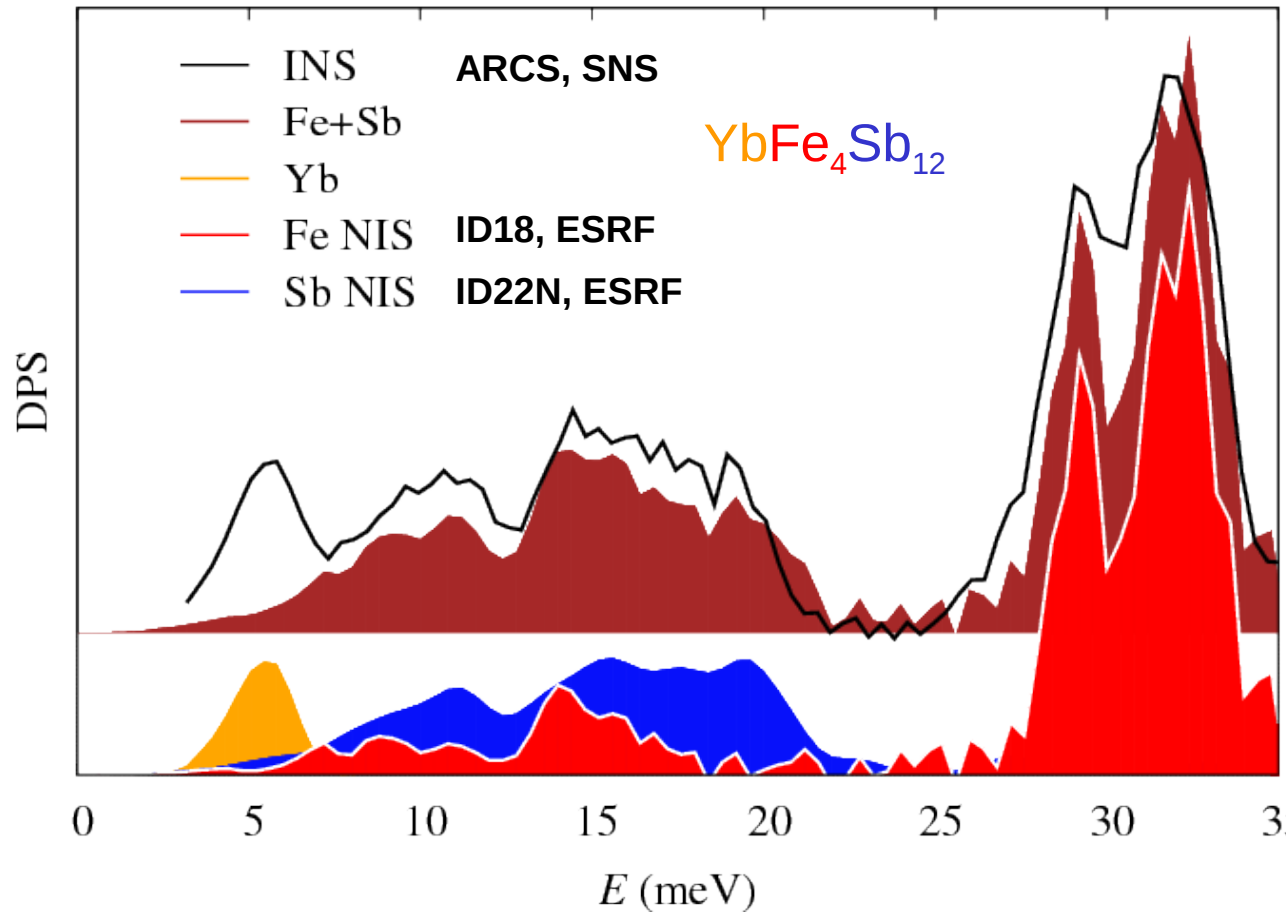


→ no structural or magnetic phase transition

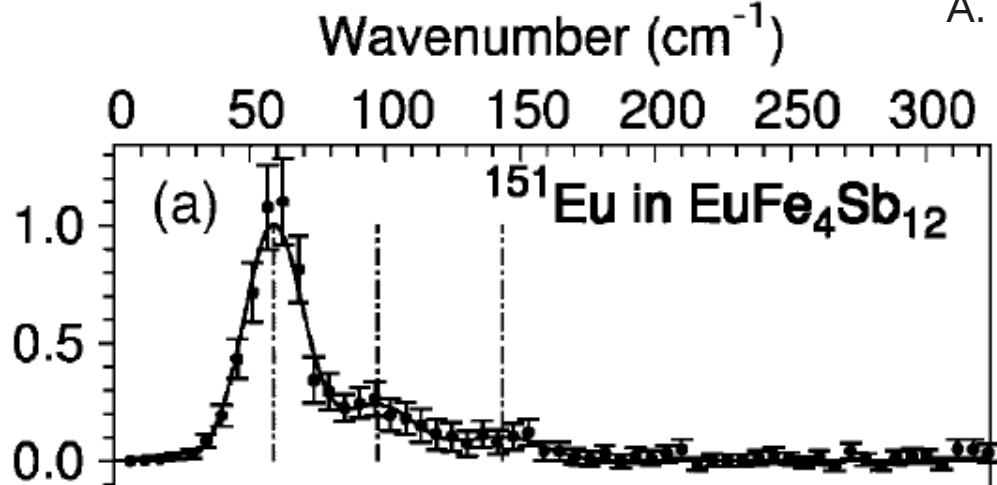
Alleno *et al.*, *Physica B: Condensed Matter* **77** (2008)

Ikeno *et al.*, *JPSJ* **76** (2007)

Density of phonon states

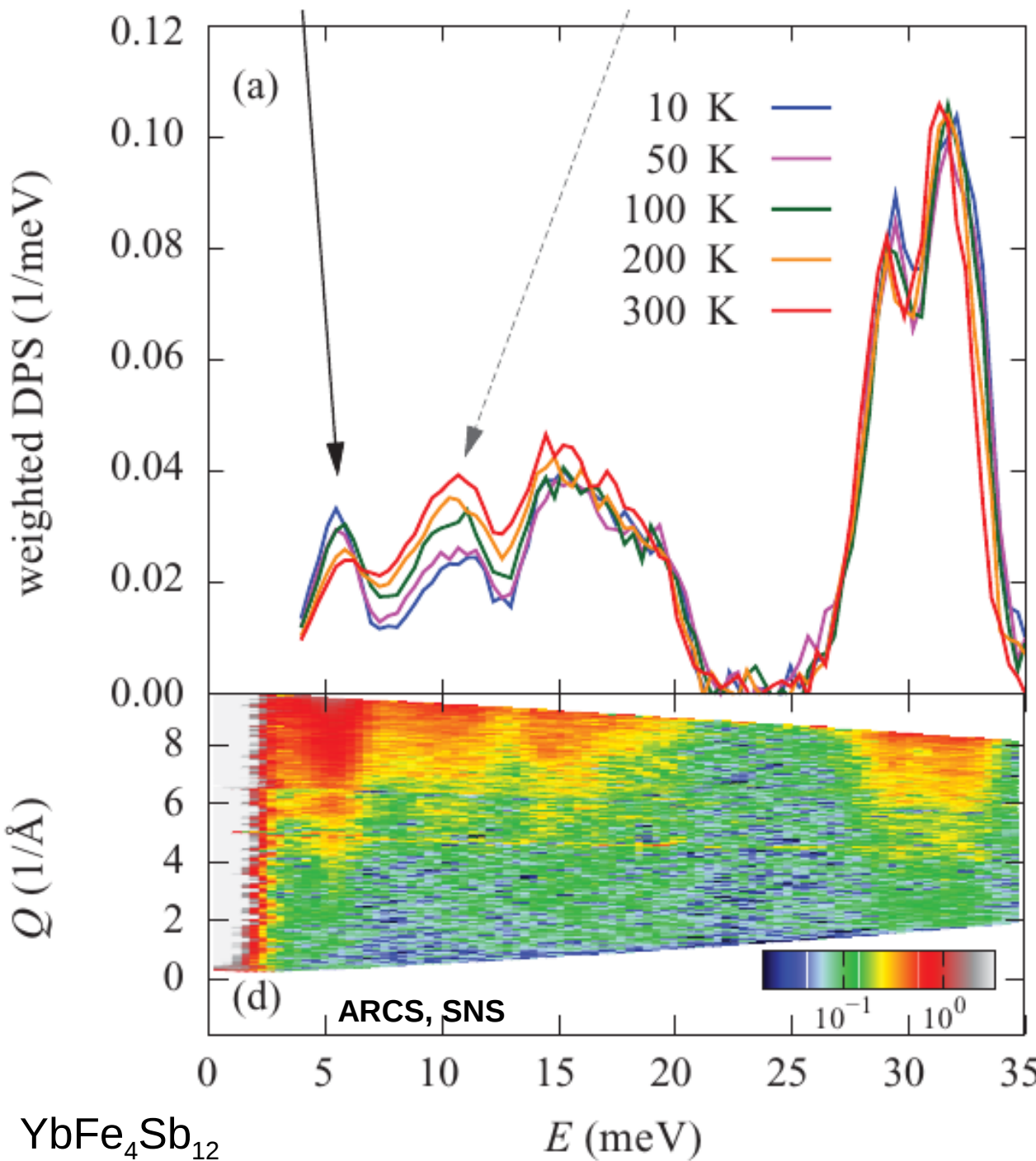


A. Möchel et al. Phys. Rev. B **84**, 184306 (2011)

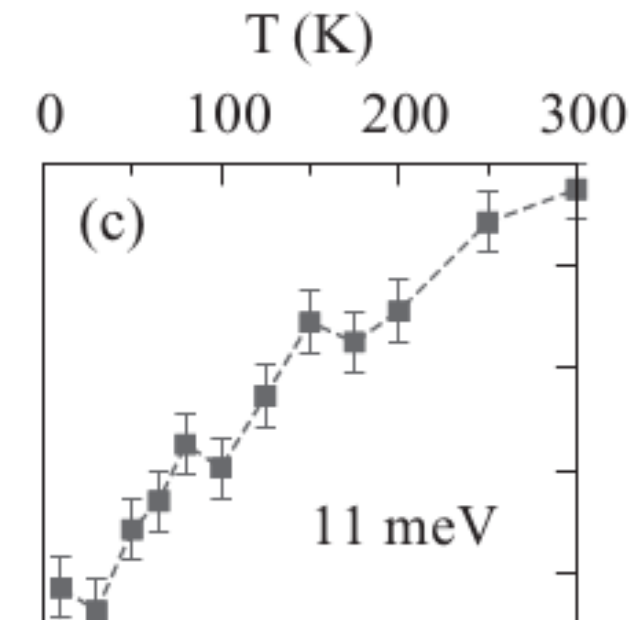


G. Long et al. Phys. Rev. B **71**, 140302R (2005)

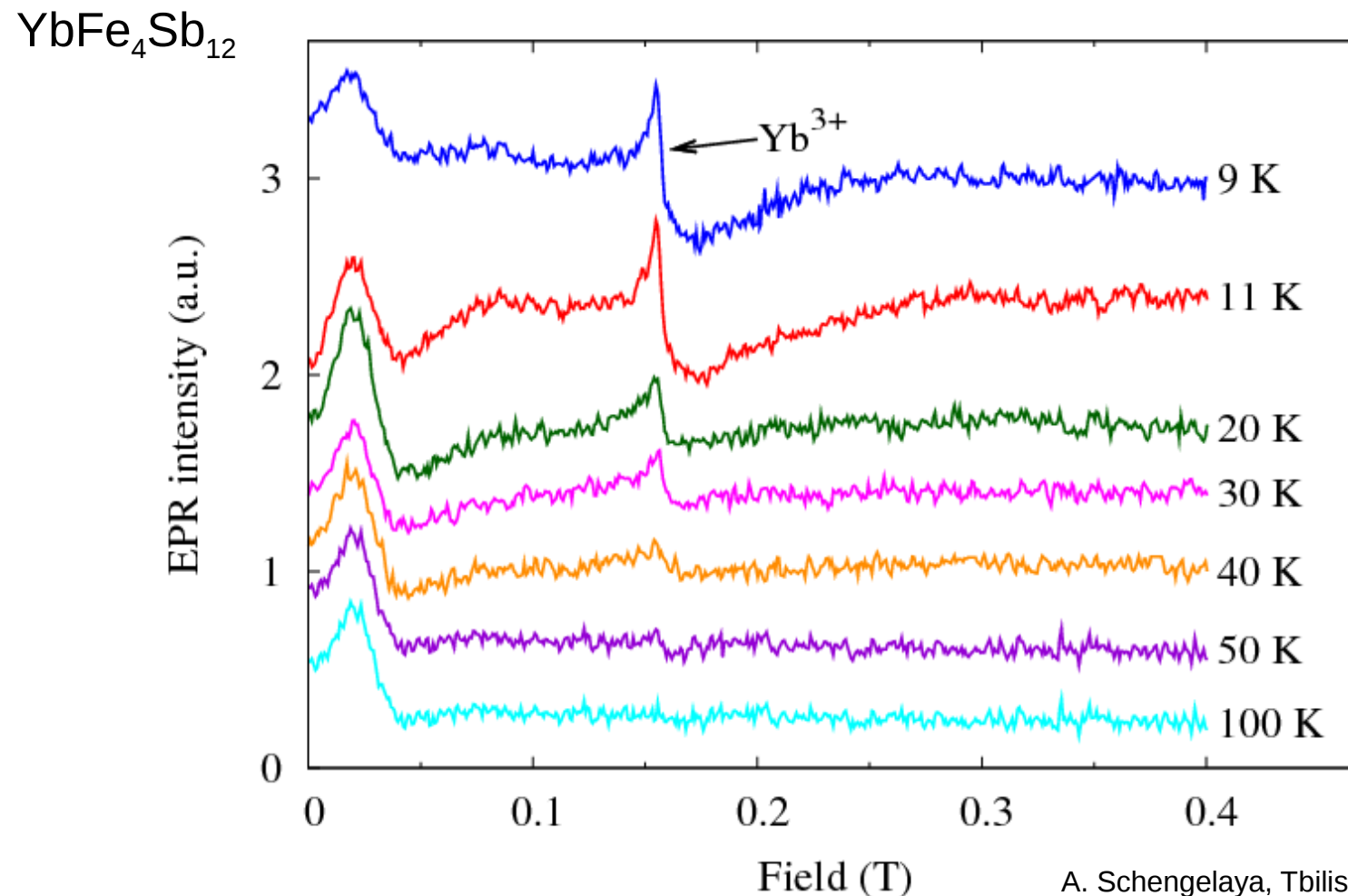
Frequency shift?



- **no shift** of the guest energy
- rearrangement of the spectral weight



Valence change



A. Schengelaya, Tbilisi State University

→ partial change of the Yb valence (?)

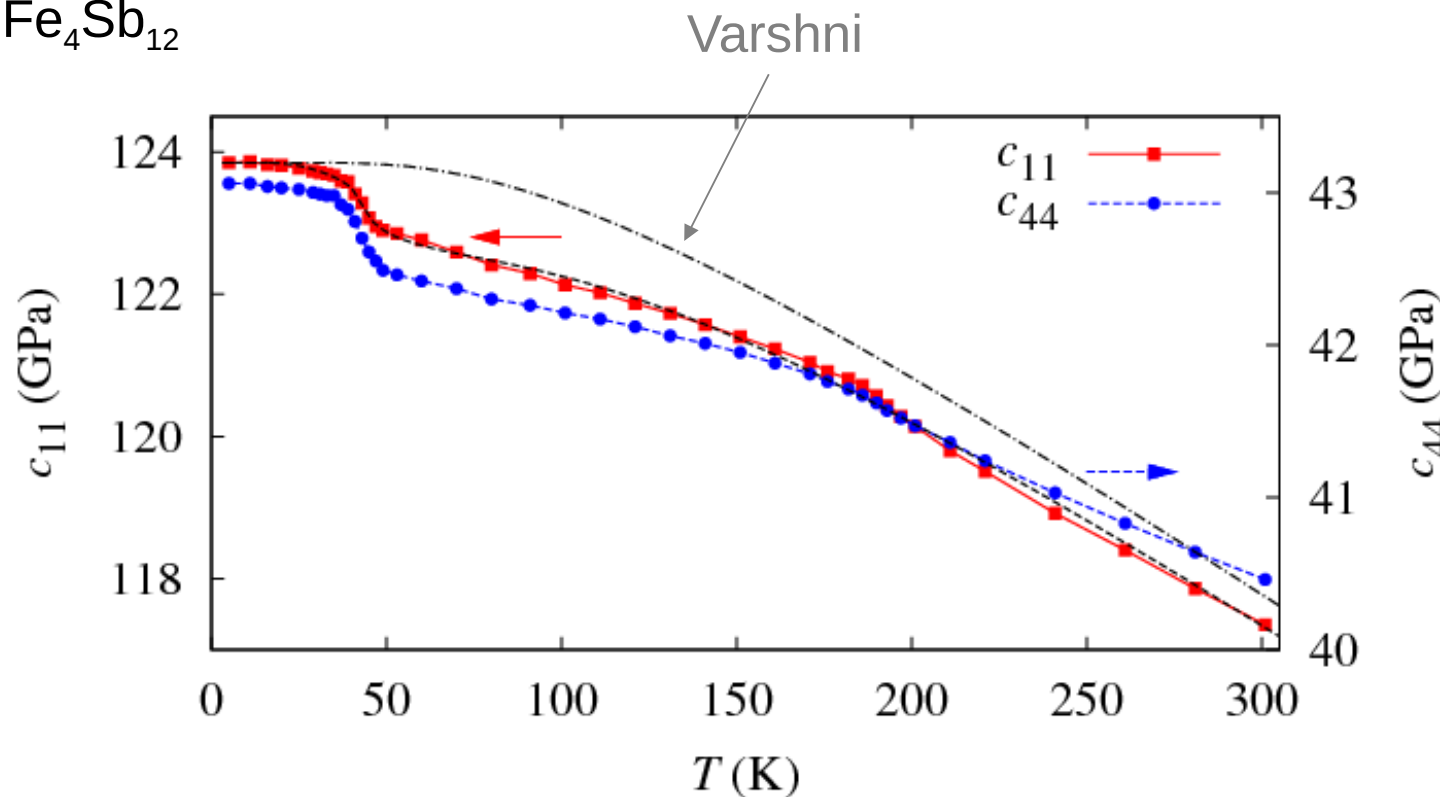
Dilley *et al.*, Phys. Rev. B **61** (2000)

Schnelle *et al.*, Phys. Rev. B **71** (2005)

Dedkov *et al.*, Physica C **460-462** (2007)

Resonant ultrasound spectroscopy

$\text{YbFe}_4\text{Sb}_{12}$



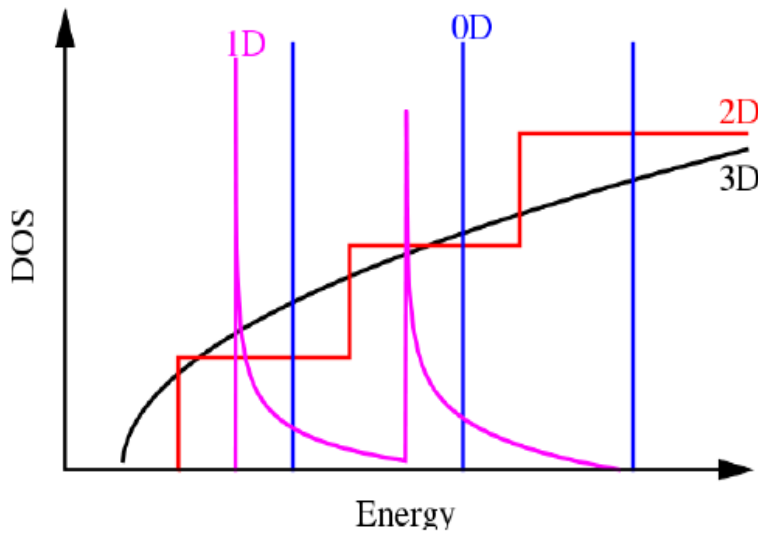
V. Keppens, University of Tennessee

- ✖ structural phase transition
- ✖ magnetic phase transition
- ✖ shift of the guest atom frequency
- ✓ Yb valence change → has to be confirmed (e.g. by XPS)

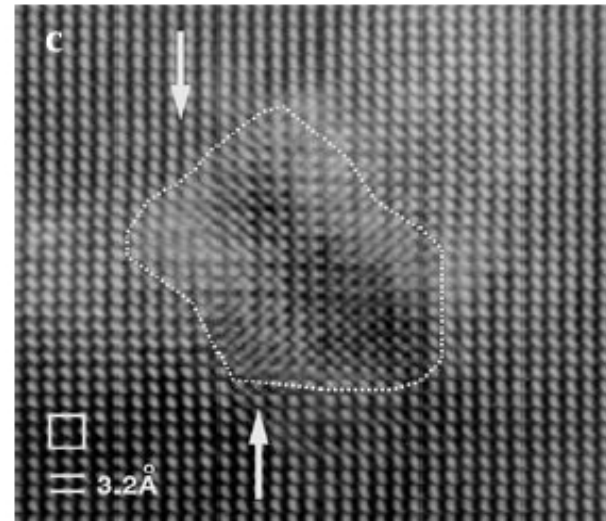
Nanostructured thermoelectrics

Key idea (Hicks, Dresselhaus, 1992):

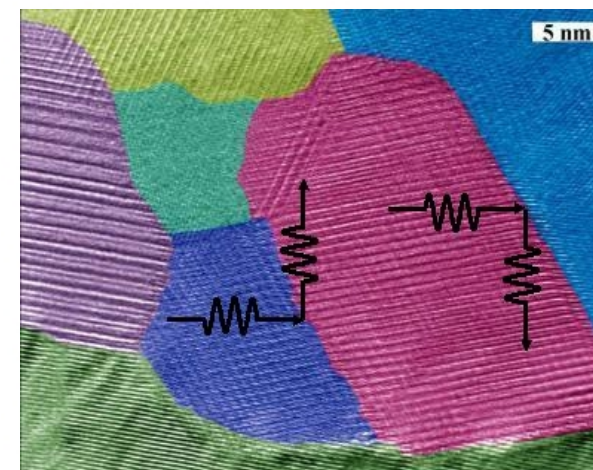
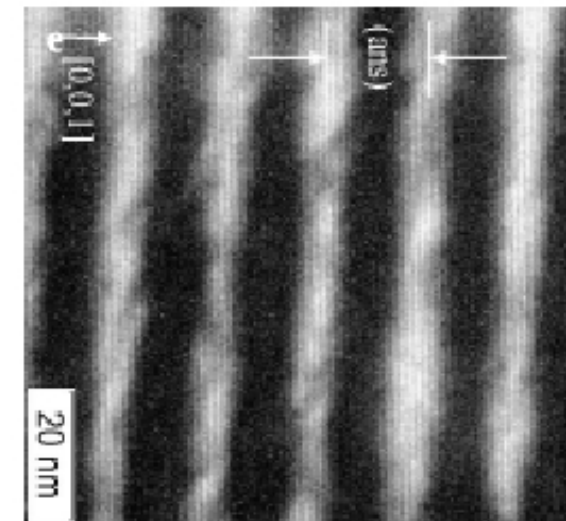
Electronic band engineering
and phonon blocking



Embedded nanodots
(Kanatzidis group)



Artificial nanostructures
(N. Peranio, PhD diss., U. Tübingen)



Nanocomposites
(Poudel et al., Science 2008)



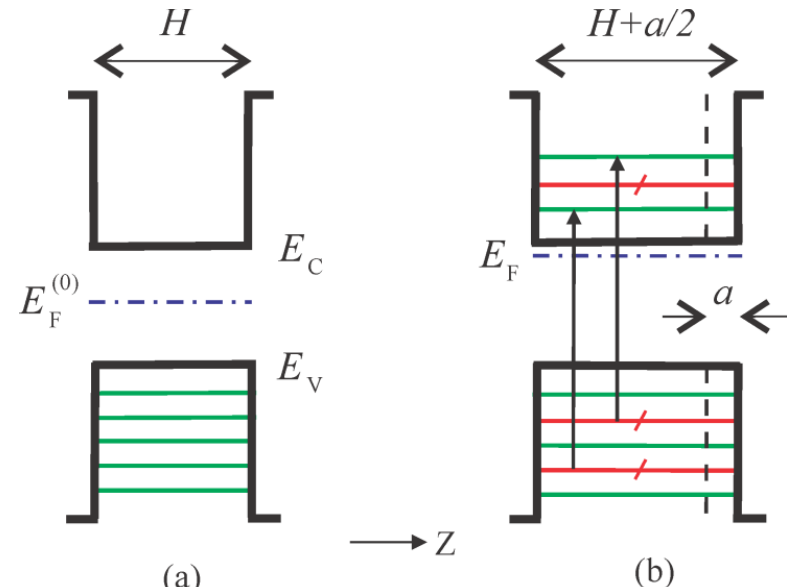
Self organization
(Gorsse et al., Chem. Mater. 2009)

Thermoelectric properties of nanogratings

Key idea: geometrically modulated density of electronic states (DOS)

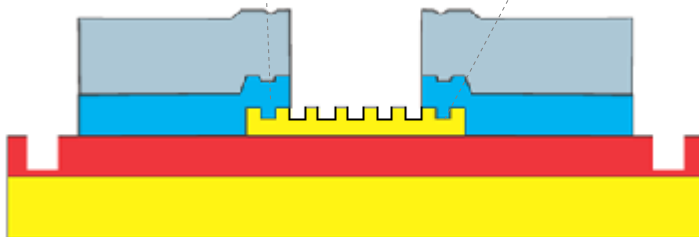


Nanoscale patterning that matches the electron De Broglie wavelength



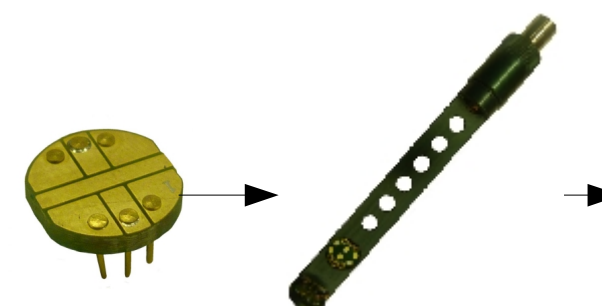
Prof. Avtandil Tavkhelidze, ISU
M. Sc. Michael Mebonia ISU and FZJ

→ Tuning of the thermopower, the derivative of the DOS at the Fermi level



Fabrication with Extreme UV Lithography
and in the future at the Helmholtz Nano Facility

Prof. Larissa Jushkin, RWTH and FZJ



Structure and transport characterization:
Scattering (JCNS, GALAXI) and cryomagnet

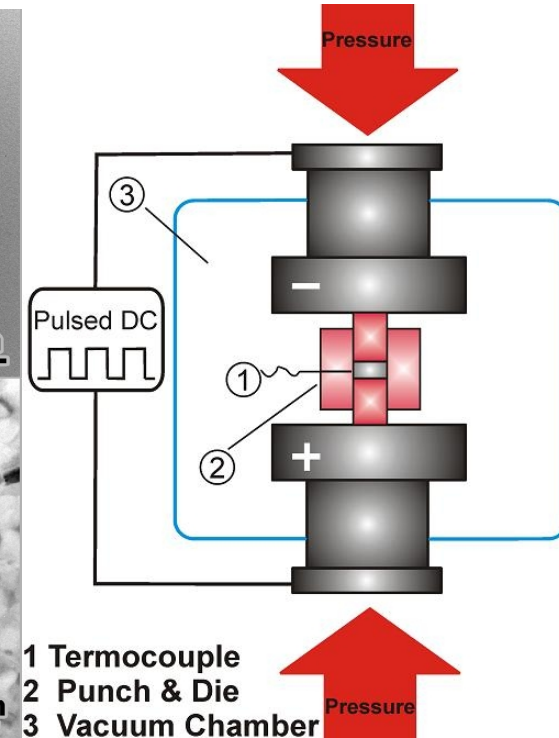
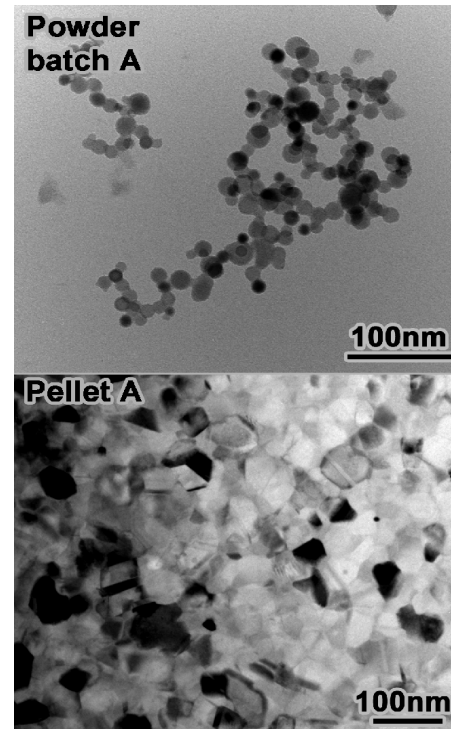
Prof. Raphaël Hermann, FZJ and Liège

Nano Si (P-doped) preparation

- Gas phase synthesis with hot wall reactor and plasma-assisted microwave reactor

Source: cpfs.mpg.de

- Variables:
 - *microwave power*
 - *chamber pressure*
 - *concentration of precursor gases* (SiH_4 , GeH_4) + PH_3
and plasma gases Ar and H₂



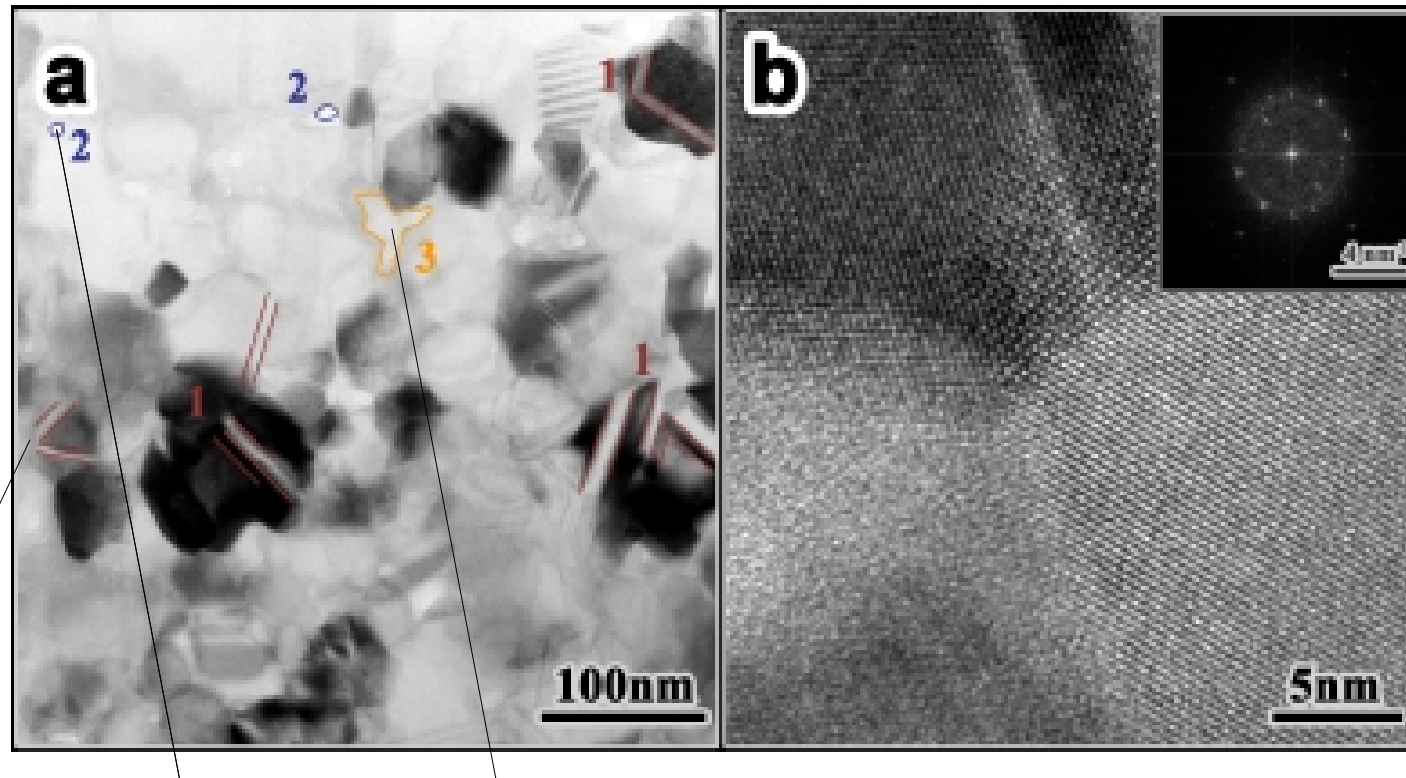
AG Schierning, U. Duisburg-Essen

- Pellets: Spark Plasma Sintering
aka *Current And Pressure Assisted Sintering*

Nanocrystalline silicon: impurities

First attempts: contains SiO_2

Briefest exposure to air between production and sintering → oxidation

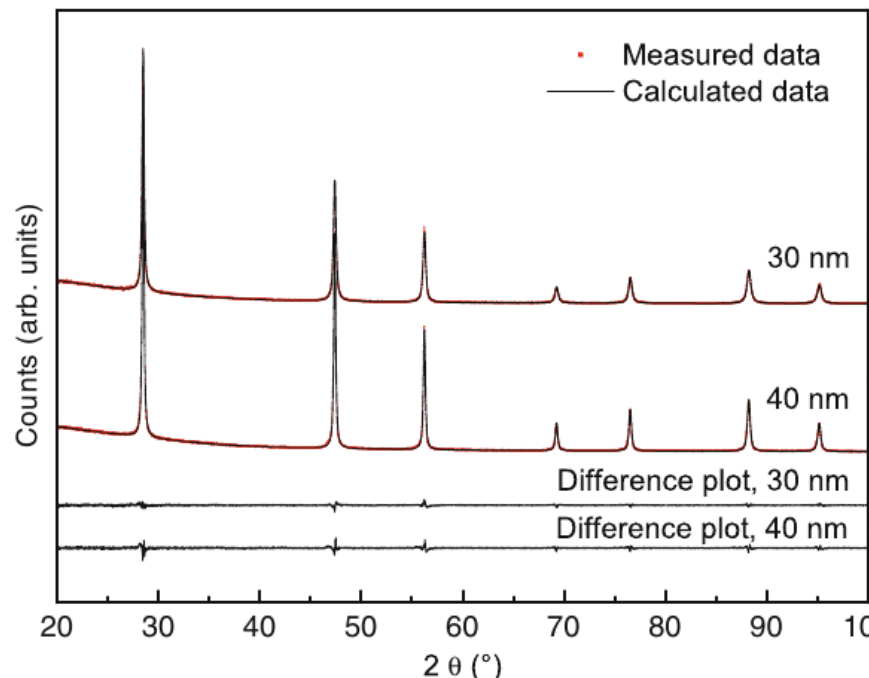


Twins

Pores

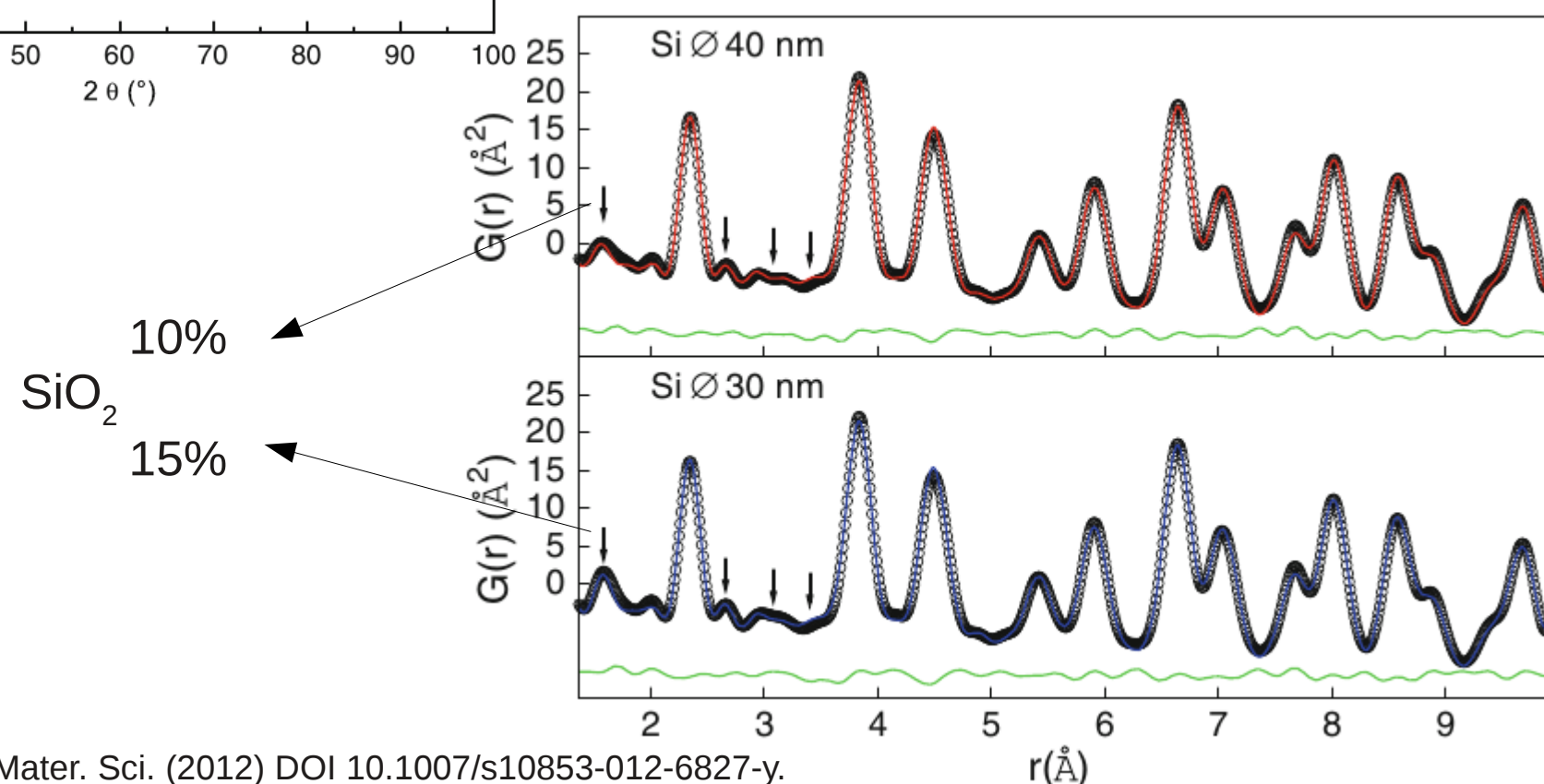
Oxidic precipitates

Diffraction and pair distribution function

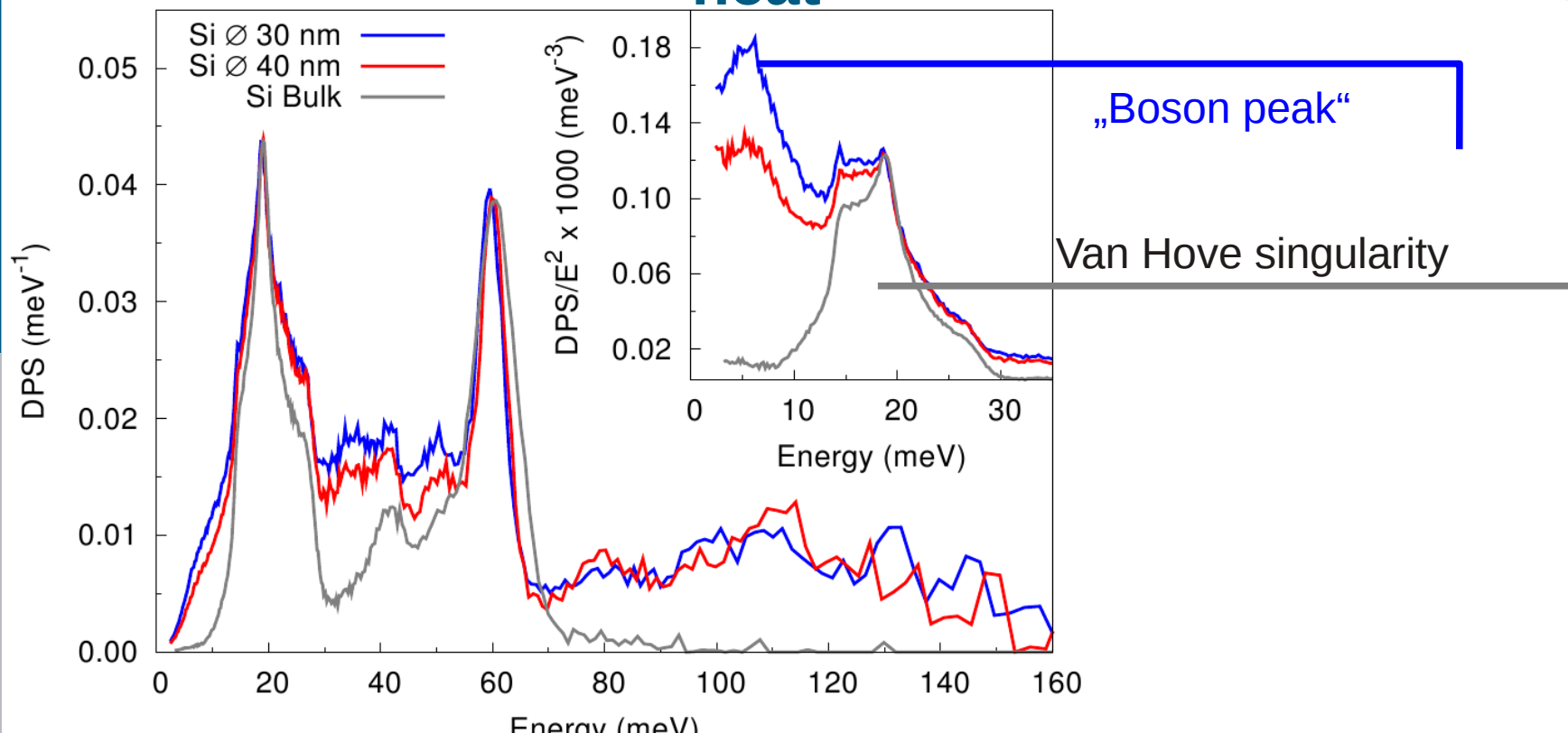


Phase pure ?

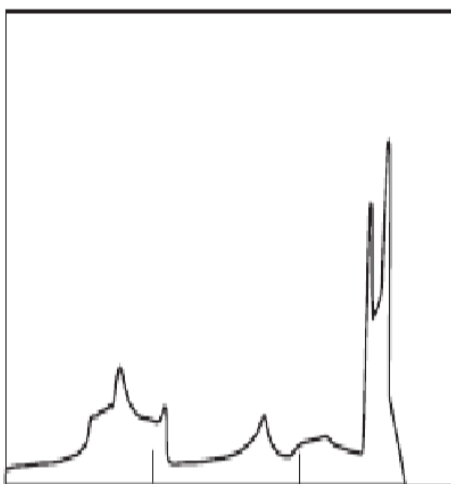
PDF, JCNS 6-ID-D, APS



Nano-Si Inelastic neutron scattering and specific heat

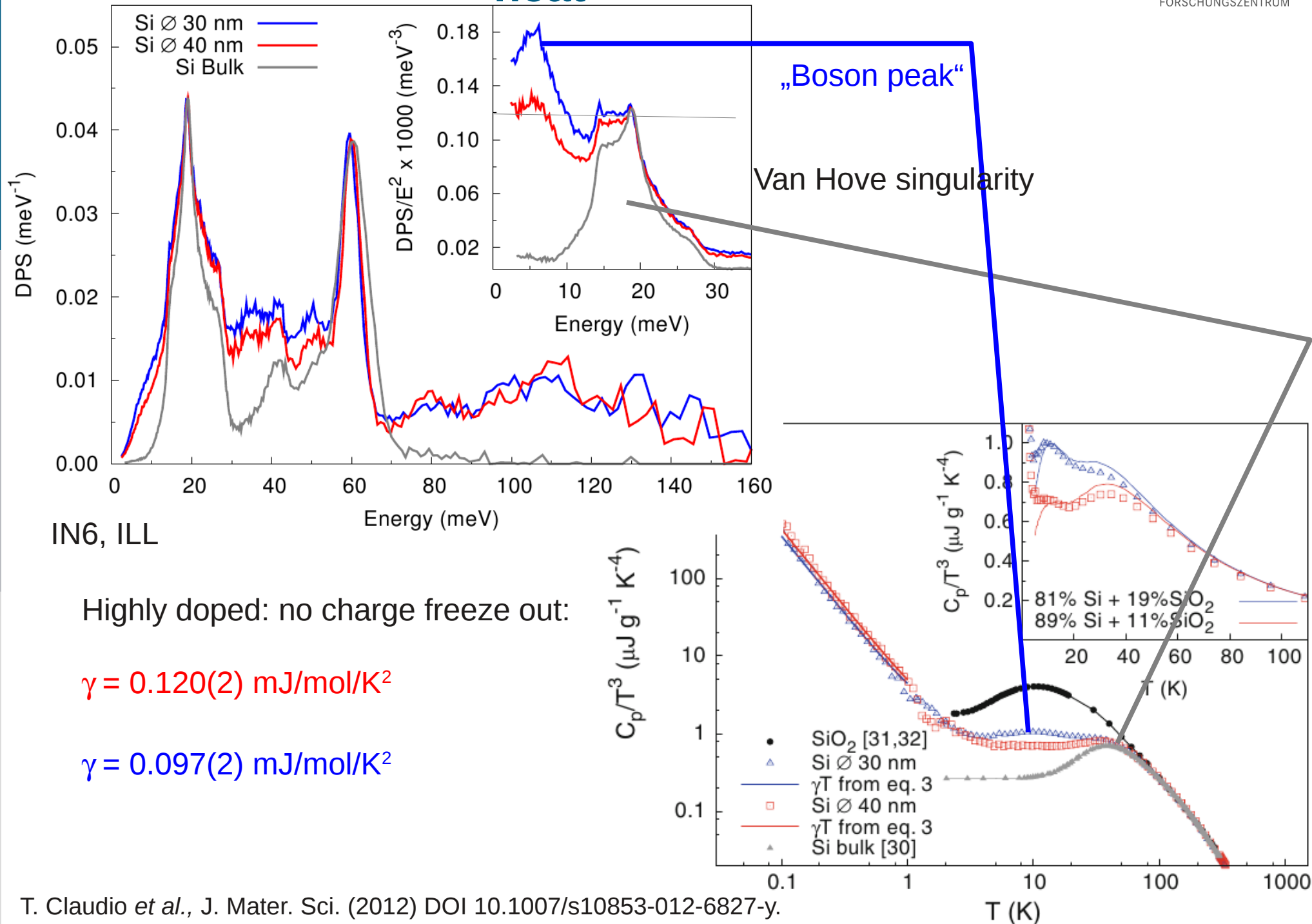


IN6, ILL



- No obvious peak broadening
- **Impurity signatures:** SiO_2 + Si-H stretching

Nano-Si Inelastic neutron scattering and specific heat



Nanocrystalline silicon – controlling purity

Functionalisation by hydrogen to avoid oxidation

Inert conditions at all steps

Sintering immediately after synthesis:

Heating/cooling 100 K/min

$T = 1150 \text{ }^\circ\text{C}$, $P = 35 \text{ Mpa}$

Sample A: 14 nm initial, 3 minutes

Sample B: 52 nm initial, 30 minutes

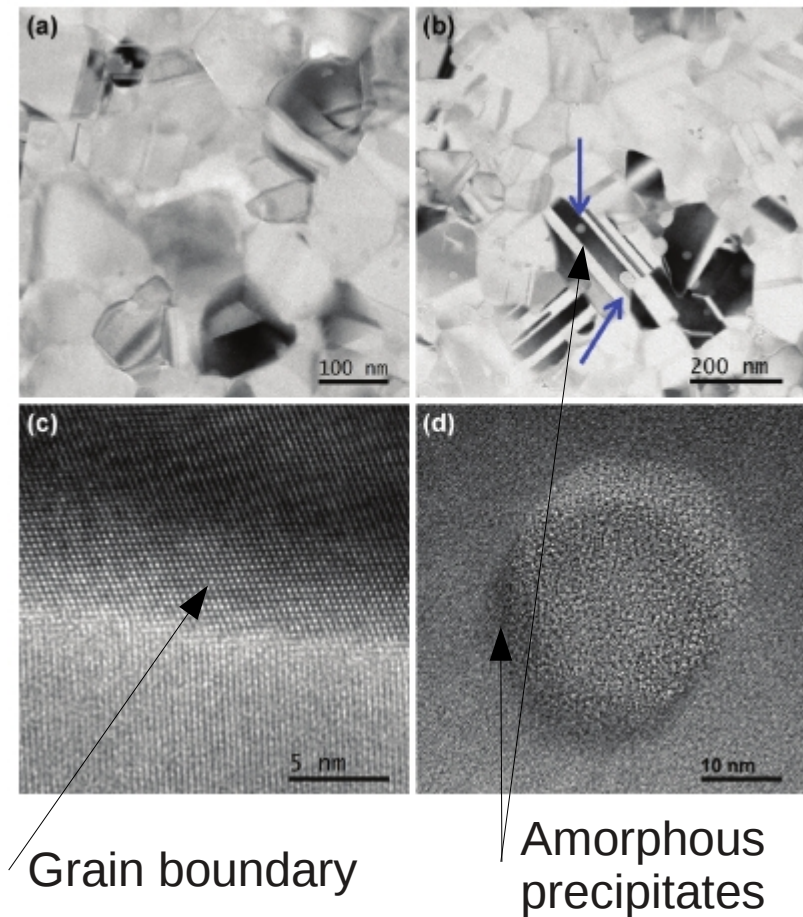
Sample C: 52 nm initial, 3 minutes

Elemental analysis at PGAA, MLZ:

99.0(1)% Si, 1.0(7)% of P dopant

H ~ 0.20(1)% in sample A

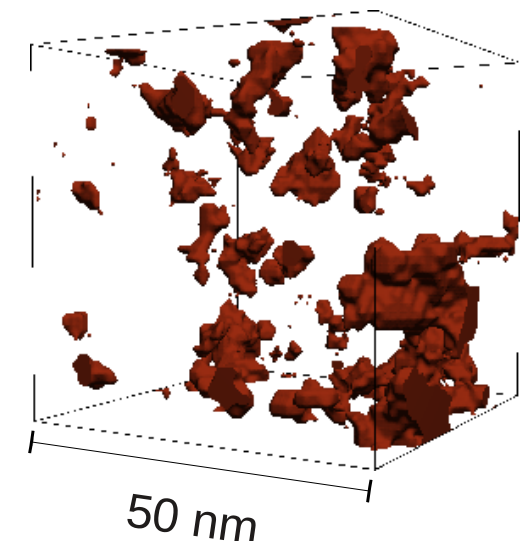
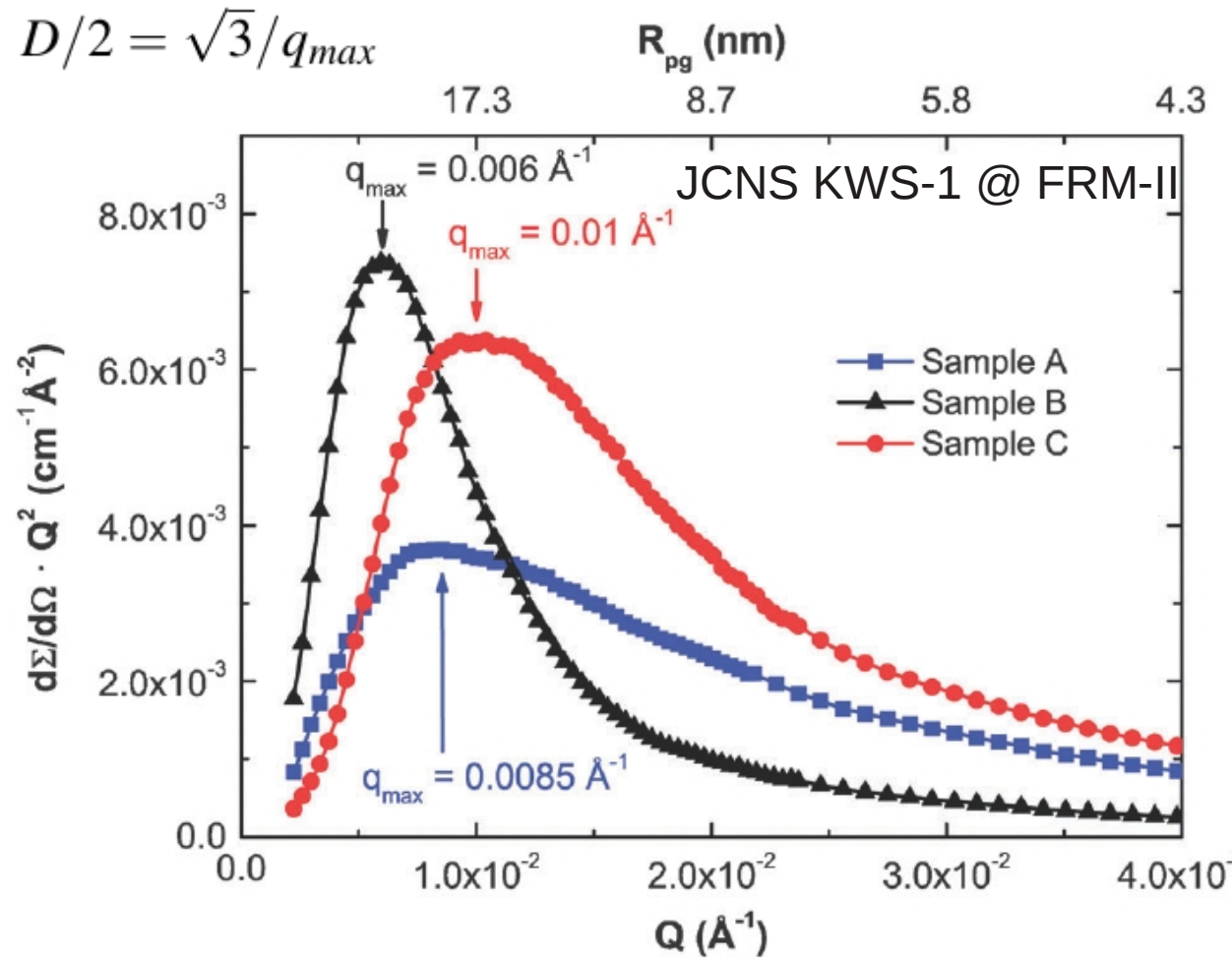
ppm B (diborane in silane precursor)



Grain boundary

Amorphous precipitates

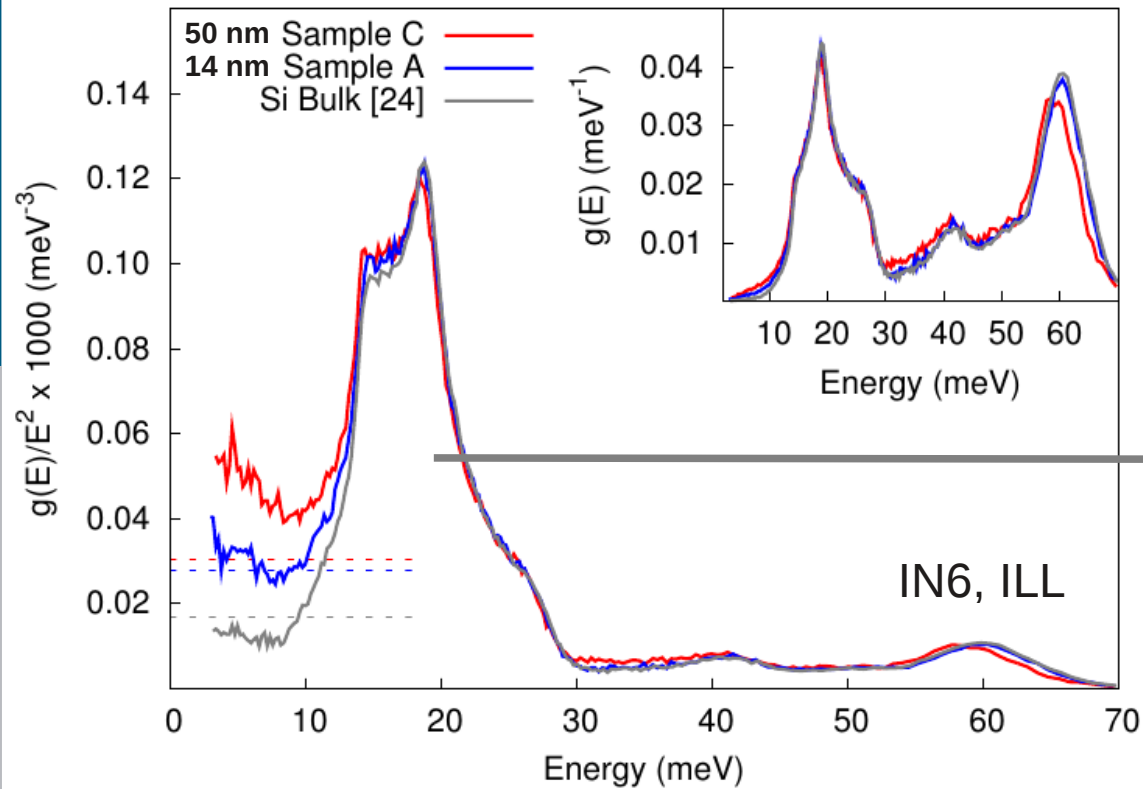
Microstructure: SANS



Representative morphology
(SAXSmorph)
„pores“ depicted in brown

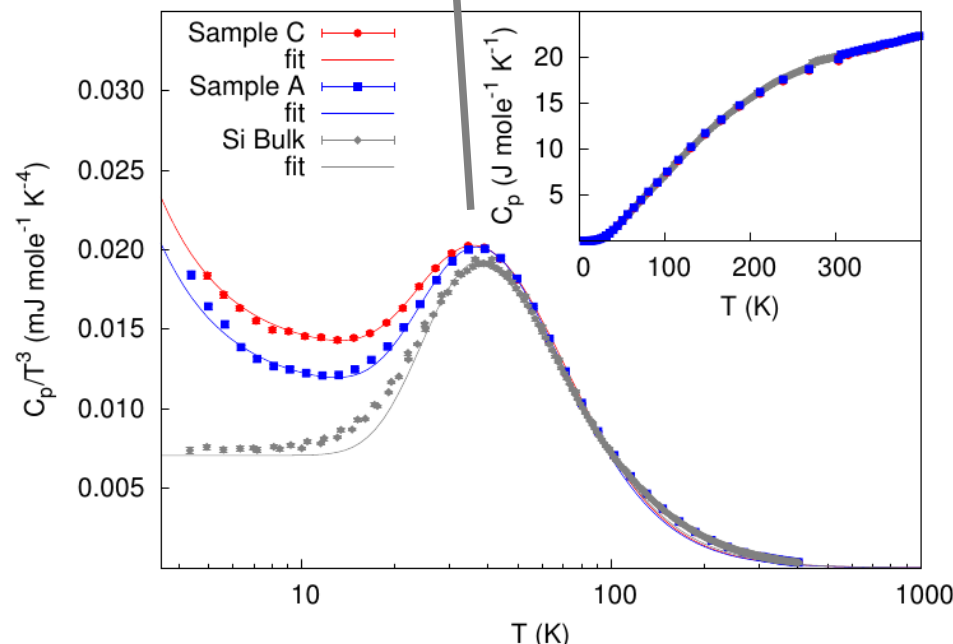
	TEM			XRD		SANS	
	D_{min} (nm)	D_{max} (nm)	D_{av} (nm)	D (nm)	ε (%)	D (nm)	
Sample A	48	264	114	40(2)	0.00138	42	
Sample B	—	—	—	42(2)	0.00133	58	
Sample C	47	246	112	33(1)	0.00150	34	

Clean samples: inelastic scattering and specific heat

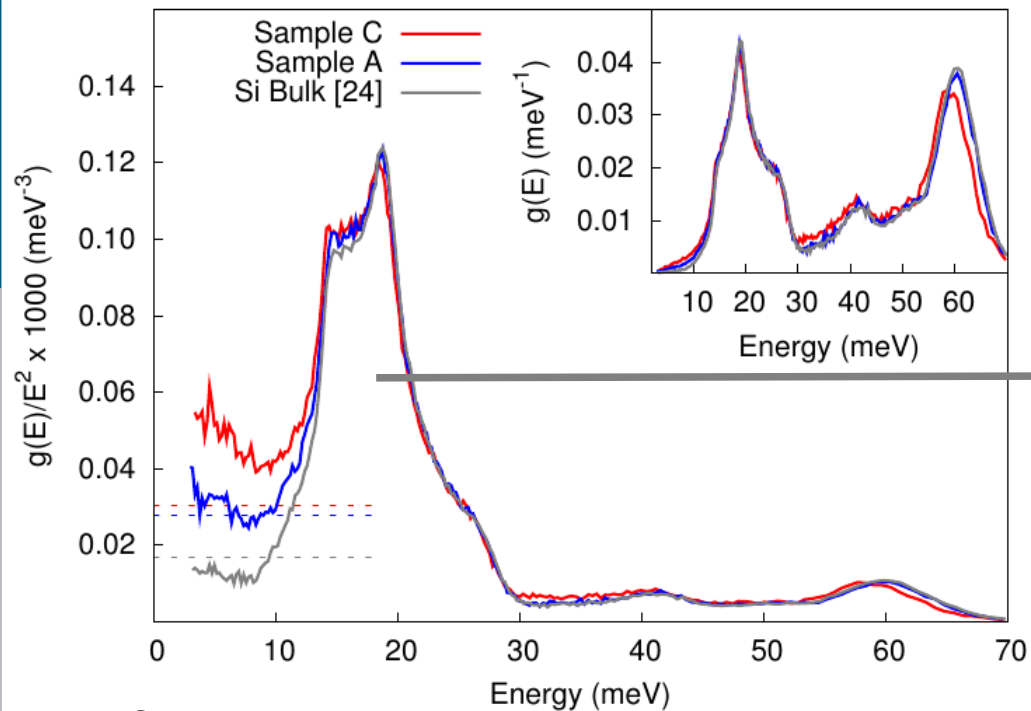


SiO_2 strongly reduced

Van Hove singularity



Clean samples: inelastic scattering and specific heat

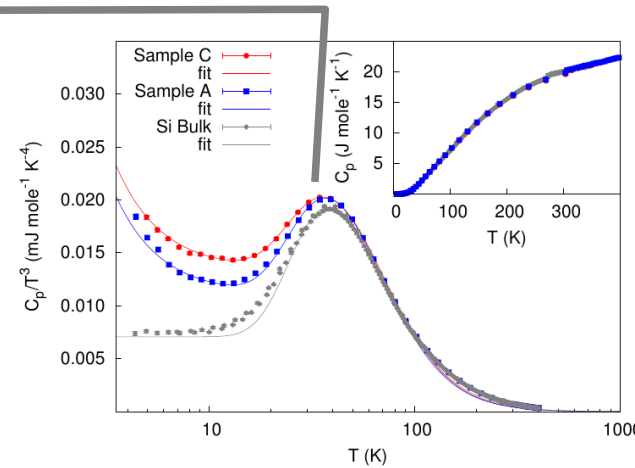


SiO₂ strongly reduced

Van Hove singularity

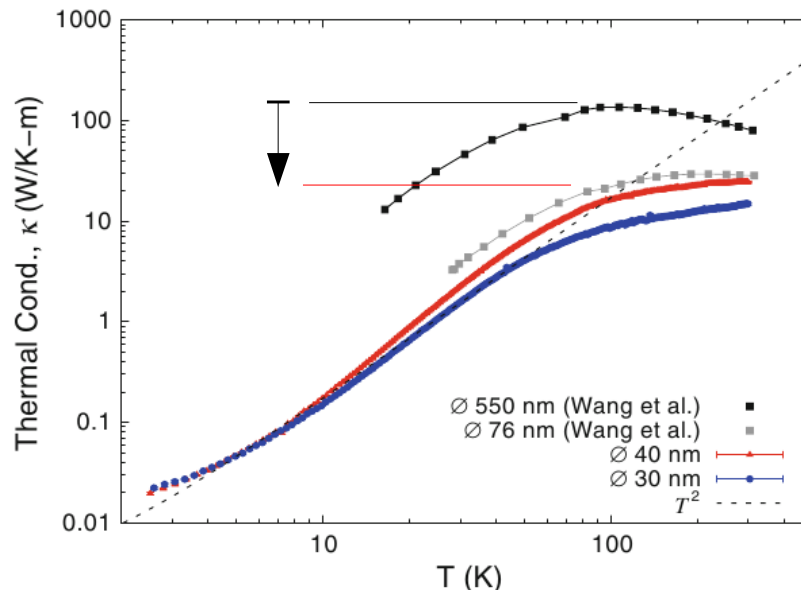
IN6, ILL

Reduced speed of sound, reduced shear modulus



	v_s (km/s)				
	C_{11} (GPa)	C_{44} (GPa)	RUS	DPS	C_p, Θ_D^{LT}
Bulk	160.1 ³²	80.0 ³²	5.94	6.73(5)	5.70(5)
Sample A	173(3)	59.0(8)	5.0(1)	5.0(3)	4.44(9)
Sample C	172(3)	58.2(7)	4.9(1)	4.3(3)	4.2(1)

Thermoelectric properties



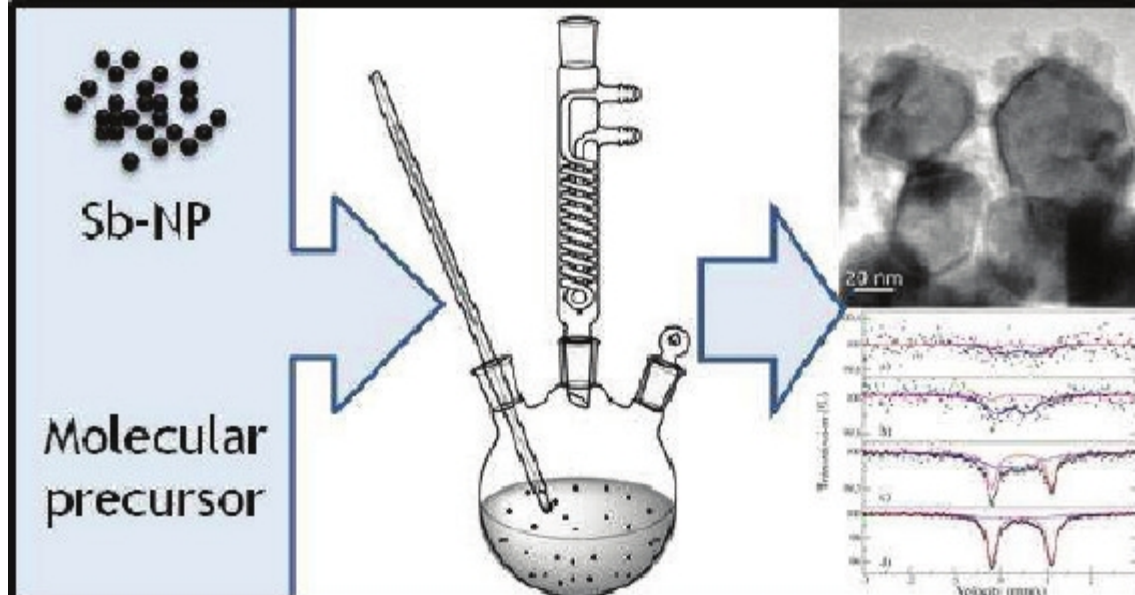
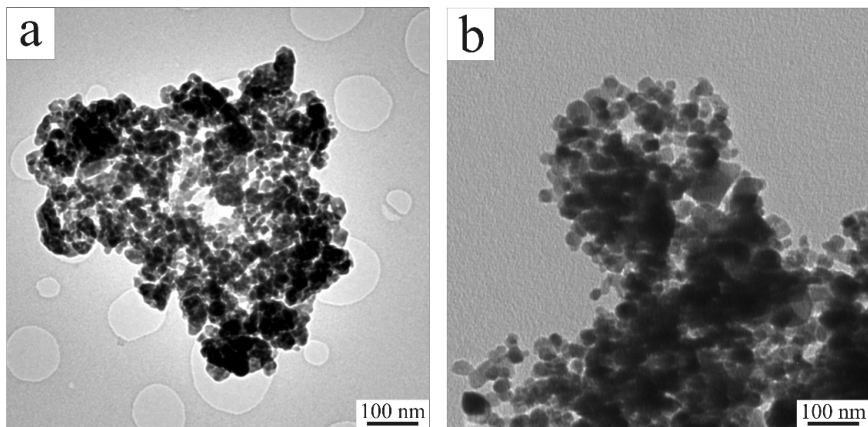
	Single-cryst.	Nanocryst. ³⁷	Nanocryst. ²⁴	Sample A	Sample B	Sample C
Nanoparticles production	-	Ball-milling	Gas phase synthesis		Gas phase synthesis	
SPS temperature (°C)	-	-	1050	1150	1150	1150
SPS hold time (min)	-	-	3	3	30	3
Additives / Impurities	-	(from ball-mill)	P, SiO ₂ , H	P	P	P
Av. nanocryst. size (nm)	-	50-100	30	42	58	33
<i>S</i> (μV/K)	-86	-70	-81.2	-94.3	-116	-114
<i>ρ</i> (μΩ-m)	27.3	9.1	23.7	9.3	11.0	13.2
<i>κ</i> (W/K-m)	101.6	7.0	14.8	25.0	27.2	21.9
<i>S</i> ² <i>σ</i> (mW/K ² -m)	0.3	0.5	0.2	1.4	0.8	1.0
ZT at RT	0.008	0.023	0.0055	0.017	0.009	0.014
ZT _{max} at 980°C	-	0.68	-	0.57	0.43	0.52

Wang XW et al. (2008) Appl Phys Lett 93(19):193121.

[37] Bux S et al. (2009) Adv Funct Mater 19(15):2445.

[24] T. Claudio *et al.*, J. Mater. Sci. (2012) DOI 10.1007/s10853-012-6827-y.

Nano M_xSb_y : preparation



1. Fe, Ni, Zn precursor + Sb nanoparticles

- dispersion of metal precursor (Fe: cyclopentadienyl iron(II) dicarbonyl dimer; Ni, Zn: chloride) in tetraethylenglycol added to mixture

2. Solutions were cooled down to RT

3. Reaction products collected by centrifugation

4. Washed with ethanol and dried

Coll. W. Tremel, U Mainz

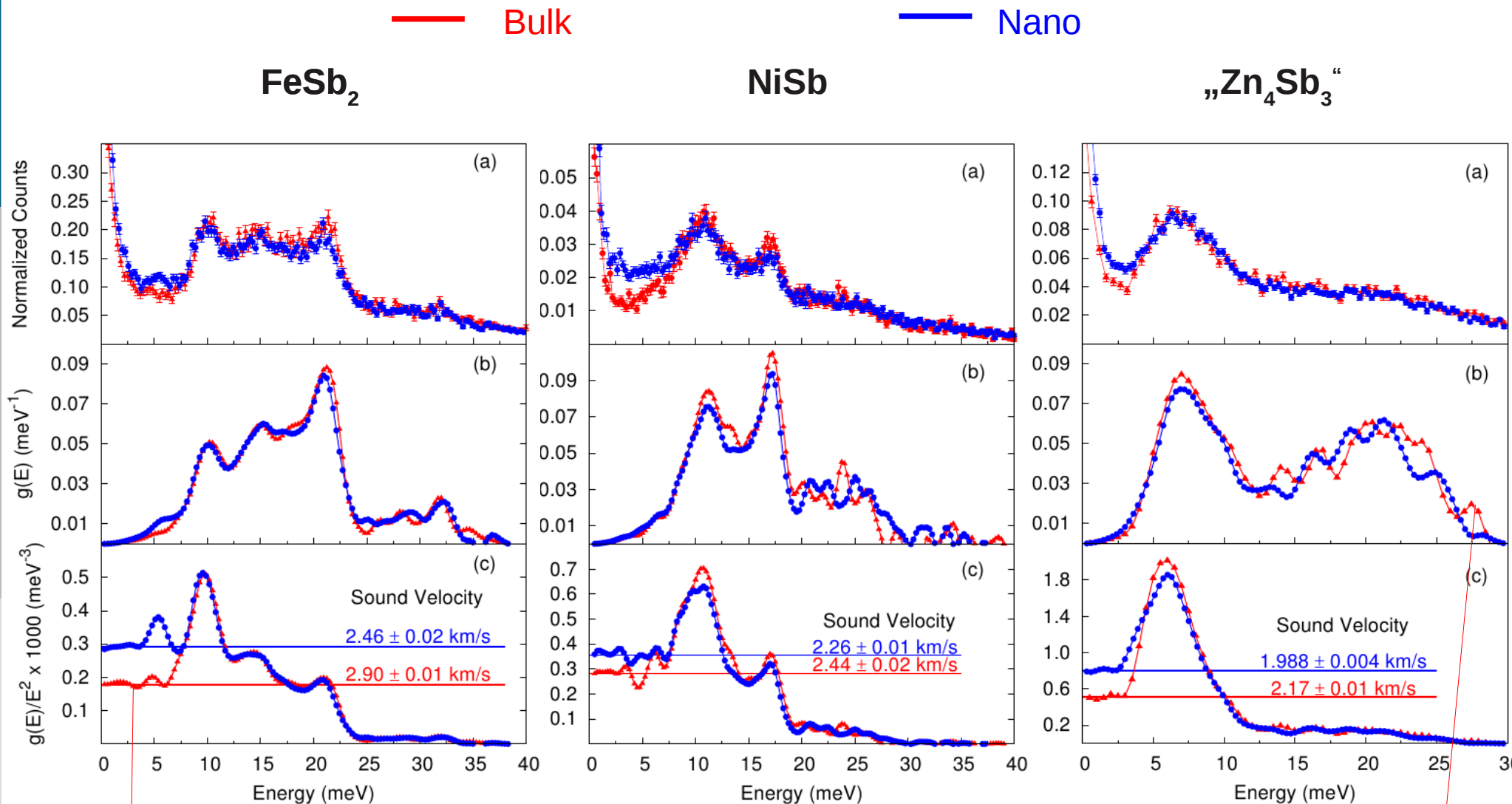
Kieslich G. et al., ChemInform, 42(39), (2011).

Birkel C. S. et al., Inorg. Chem., 50(22):11807–11812 (2011).

Birkel C. S. et al., J. Am. Chem. Soc., 132(28):9881–9889 (2010).

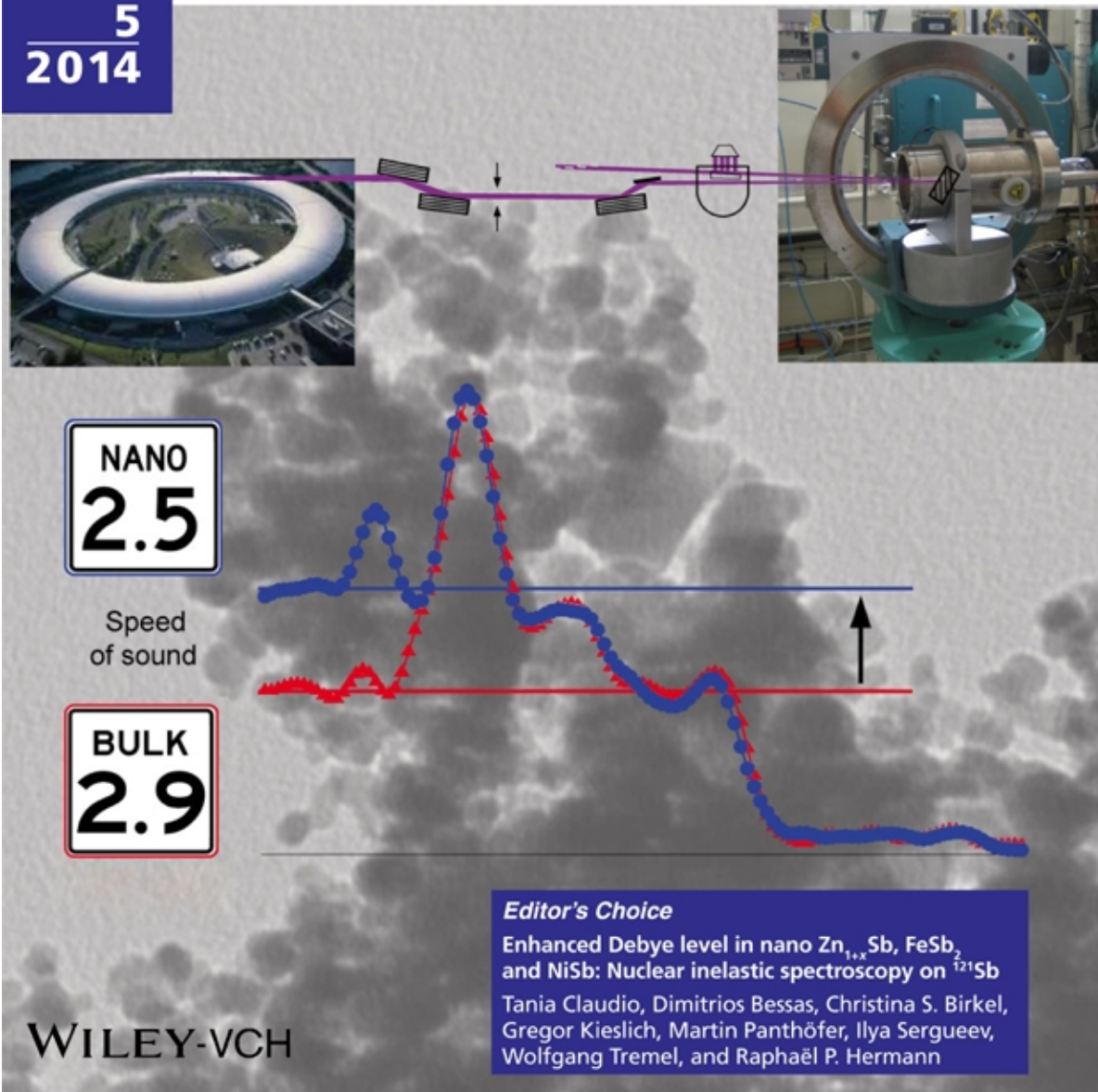
^{121}Sb phonons in bulk and nano metal antimonides

T. Claudio, PSS-B, May 8 (2014), DOI: 10.1002/pssb.201470128.

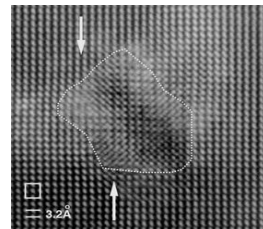


Systematic reduction of the speed of sound in the nano phases

5
2014

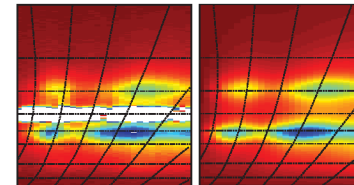
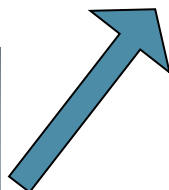


Scattering methods



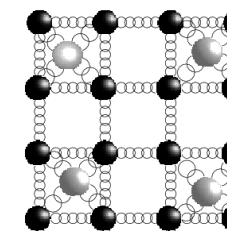
Kanatzidis et al.
JACS 2005

Materials



Understanding

Where are the atoms?
How do they move?



How does structure and dynamics affect the functionality?

Optimization



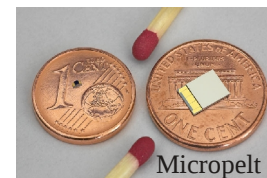
Poudel et al. Science
2008



Applications



Devices



Collaborative setting and outreach

Priority program: “*Nanostructured thermoelectrics*” DFG SPP1386
(German Universities, FhF, MPI, **DLR, GSI, KIT, FZJ**)

BMBF WING: “*Nanostrukturierte Komplexe Chalkogenide*”
(**DLR, FZJ, IOM, FhF IWM**)

German-Georgian Science Bridge “*Geometric effects in TE nanostructures*”

WE Heraeus Seminars (collab. FZJ, U Hamburg, U Duisburg-Essen, DLR, Fraunhofer IPM, U Göttingen)

- “*Nanostructured Thermoelectrics*”, 2010

“*Thermal Transport at the Nanoscale*”, 2013

“*Electrons and Phonons: Interactions and Interfaces*”, April 2016



Acknowledgments

The Helmholtz Association for funding group VH-NG 407

DFG SPP1386 „Nanostrukturierte Thermoelektrika“

BMBF WInG Initiative, Projekt 03X3540B „NanoKoCh“

DFG SFB 917 „Nanoswitches“

Large scale facilities for access: ESRF, APS, Hasylab, SOLEIL, FRM II, ILL, SNS, SINQ

Prof. K. Nielsch, U. Hamburg

Prof. O. Eibl, U. Tübingen

Dr. H. Böttner, Fraunhofer IPM

Dr. E. Müller, DLR

Prof. Th. Höche, Fraunhofer IWM

Dr. A. Neubrand, Fraunhofer IWM

Prof. Ch. Elsässer, Fraunhofer IWM

Prof. M. Albrecht, TU Chemnitz

Dr. V. Pacheco, Fraunhofer IFAM

Prof. W. Tremel, U. Mainz

Prof. M. Wuttig, RWTH Aachen

Prof. R. Dronskowski, RWTH Aachen

Dr. E. Toimil-Molares, GSI Darmstadt

Dr. G. Schierning, U. Duisburg-Essen

Prof. D. Johnson, U. Oregon

Prof. S. Kauzlarich, U.C. Davis

Prof. J. Snyder, CalTech

Dr. M. Christensen, Aarhus Universitet

Prof. A. Shengelaya, Tbilisi State University

Dr. B. C. Sales, ORNL

Prof. V. Keppens and D. Mandrus, U. Tennessee

Prof. G. Nolas, U. South Florida

Prof. L. Bergstrom, U. Stockholm

Prof. J. Gladden, U. Mississippi

Dr. R. Rüffer, Dr. A. Chumakov, ESRF

Dr. H.-C. Wille, Petra III

Dr. E. E. Alp, APS

Prof. H. Schober, Dr. M. Koza, ILL

Dr. F. Juranyi, SINQ, PSI

Prof. Avto Tavkhelidze

Prof. Larissa Jushkin



HELMHOLTZ
ASSOCIATION



JÜLICH
FORSCHUNGSZENTRUM

*Lattice Dynamics in Emerging
Functional Materials Group*



Raphaël Hermann
Group Leader



B. Klobes
Post Doc



V. Potapkin
Post Doc



A. Mahmoud
Post Doc



M. Herlitschke
PhD student



R. Simon
PhD student



M. Mebonia
PhD student

Former members



A. Houben
(Möchel)



J. Gallus



T. Rademacher



I. Sergeev



D. Bessas



P. Bauer Pereira



T. Claudio

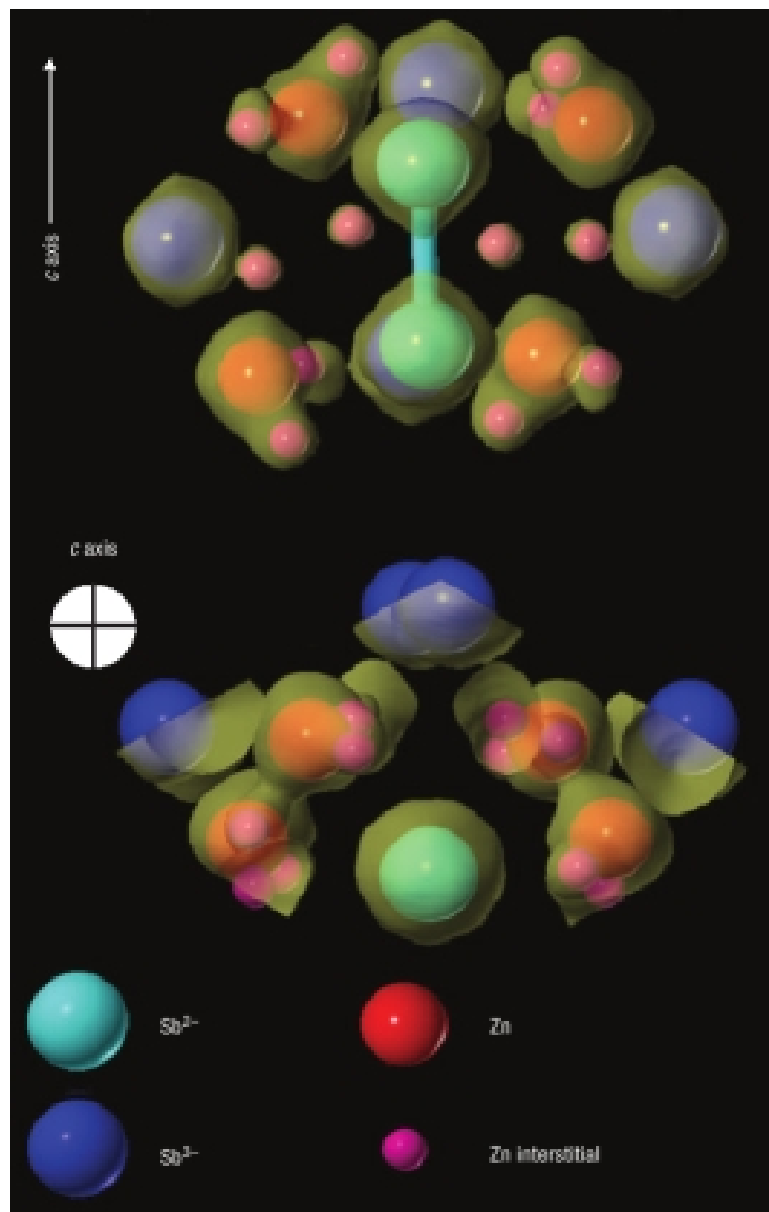
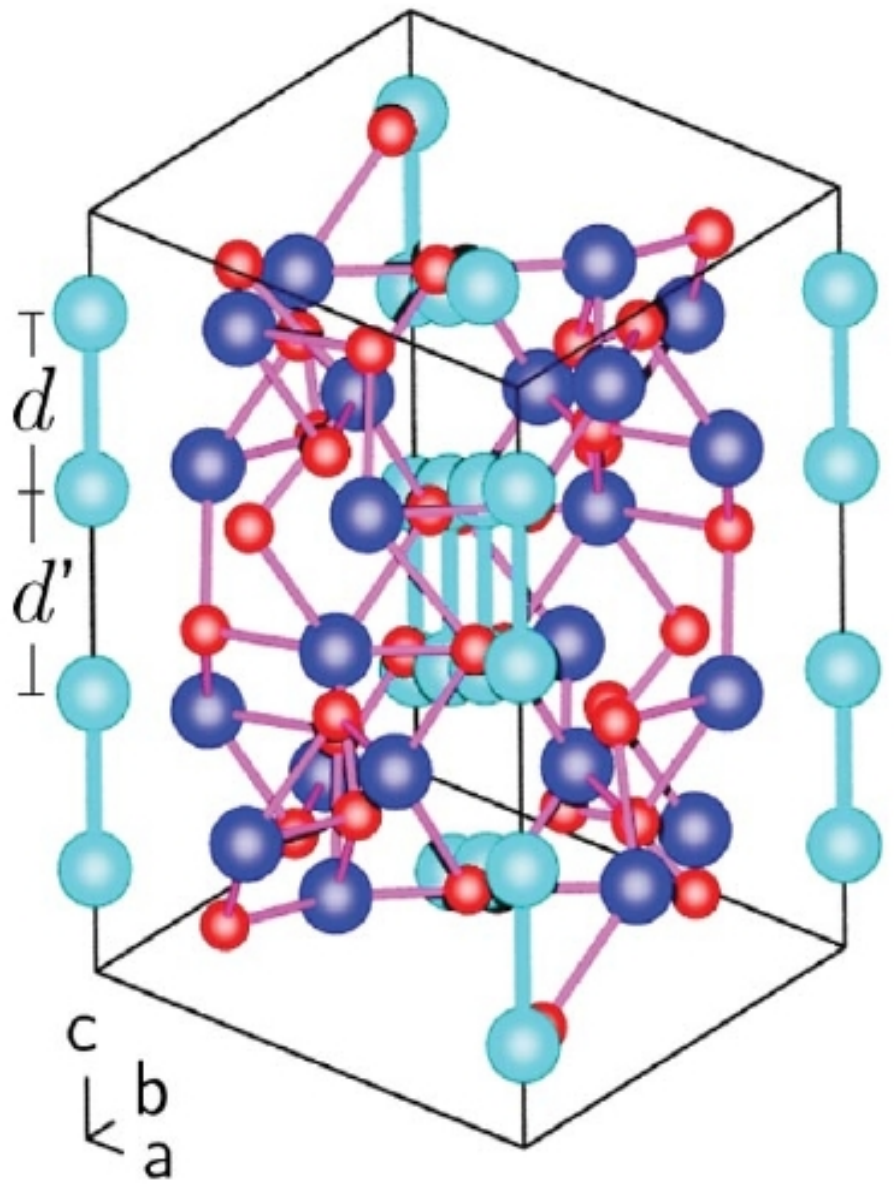


A. Jafari
PhD student



P. Alexeev
PhD student
(DESY Hamburg)

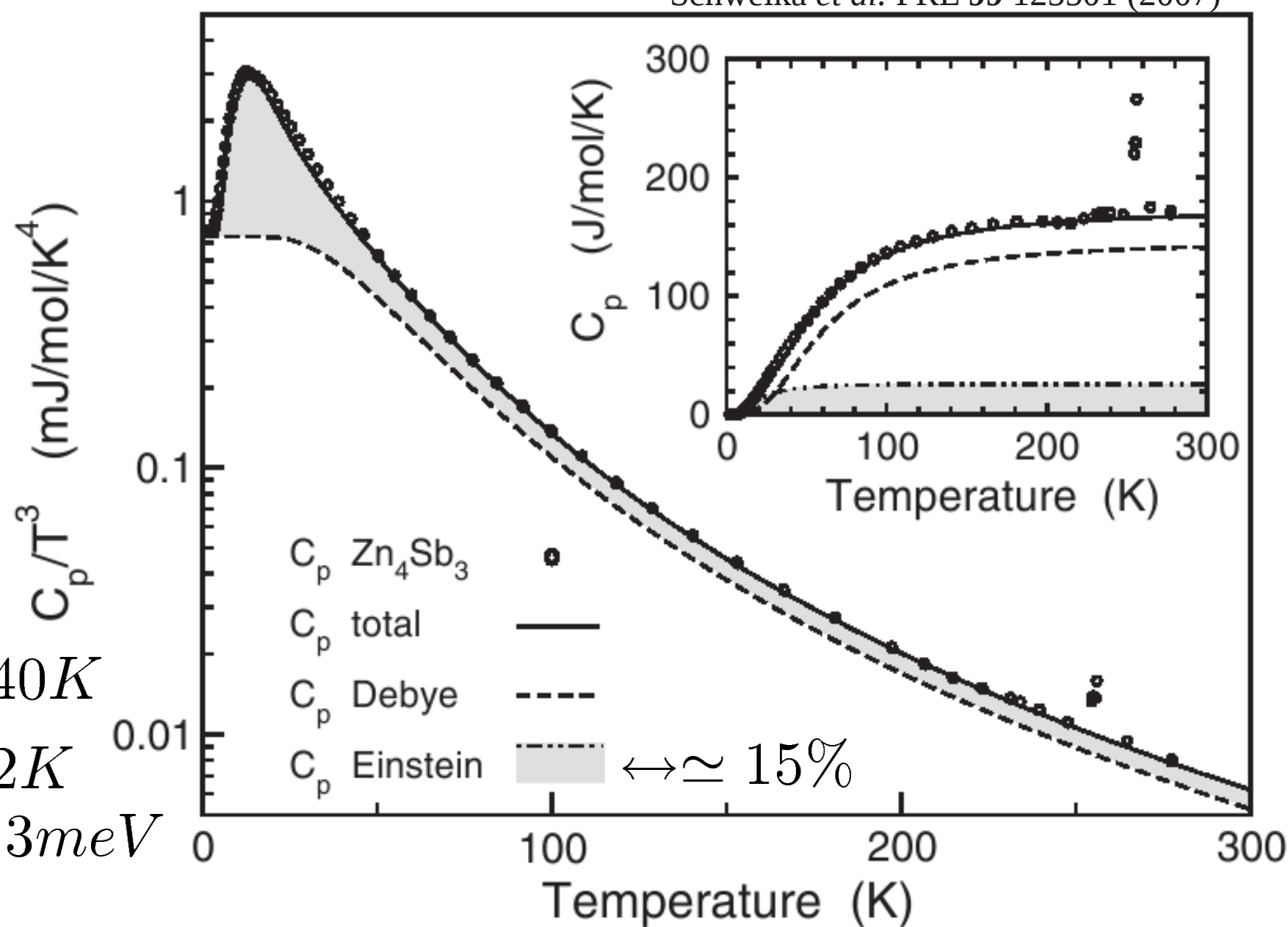
“Zn₄Sb₃” - Structure and Zn interstitials



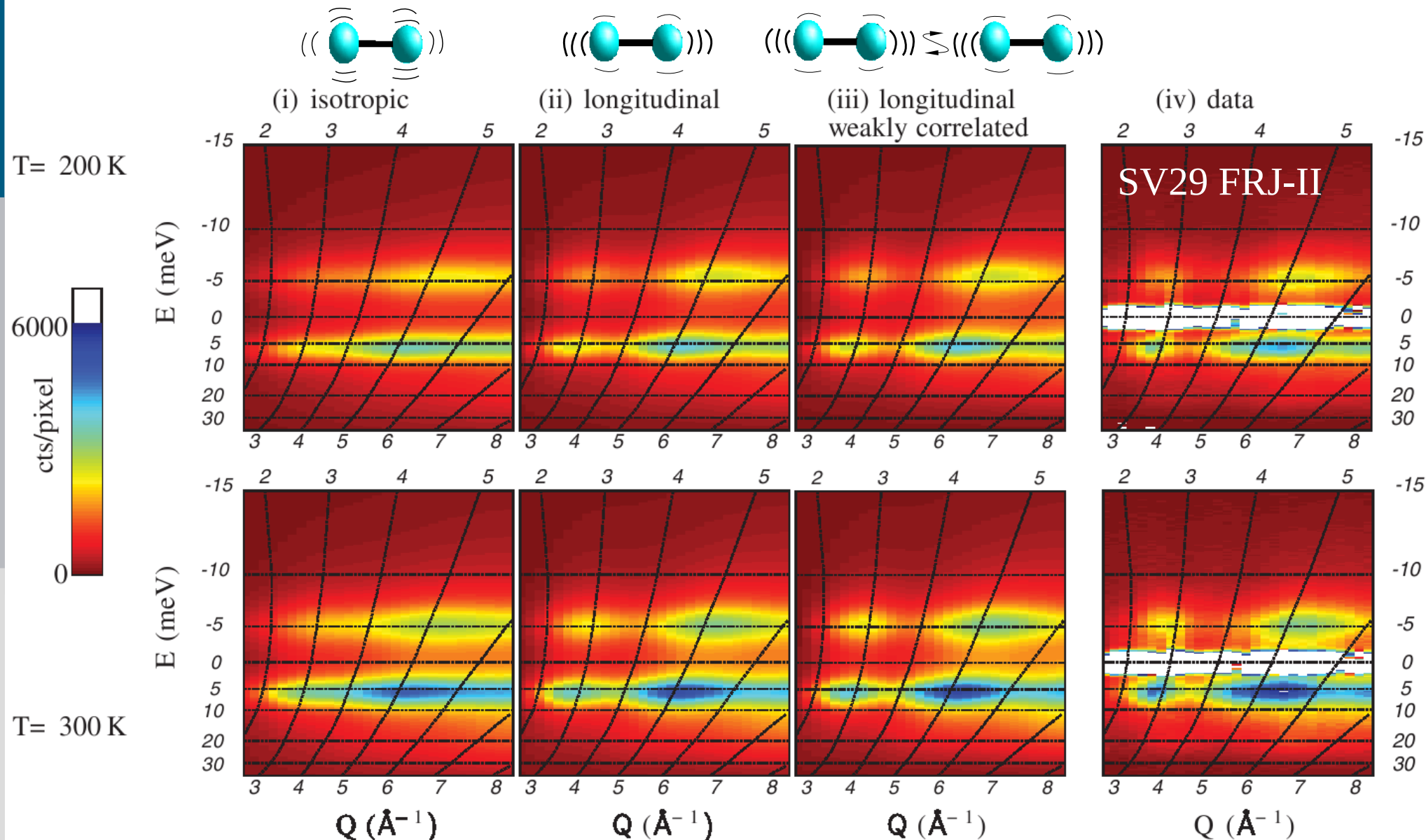
Snyder *et al.*, *Nat. Mat.* **3**, 458–463 (2004)

Zn_4Sb_3 - Heat capacity

$$\Theta_D = 240K$$
$$\Theta_E = 62K$$
$$\approx 5.3 \text{ meV}$$



Zn_4Sb_3 - Inelastic neutron scattering



Zn_4Sb_3 - Inelastic neutron scattering

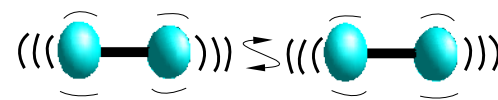
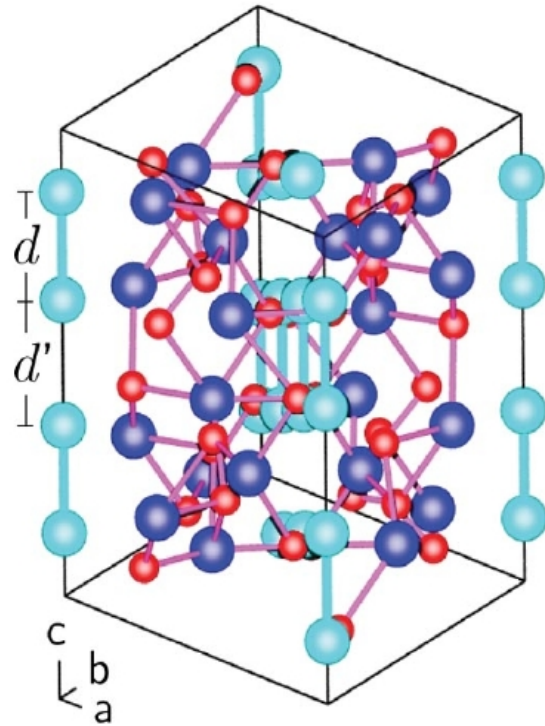
Schweika *et al.* PRL 99 125501 (2007)

$$E = 5.23(2) \text{ meV}$$

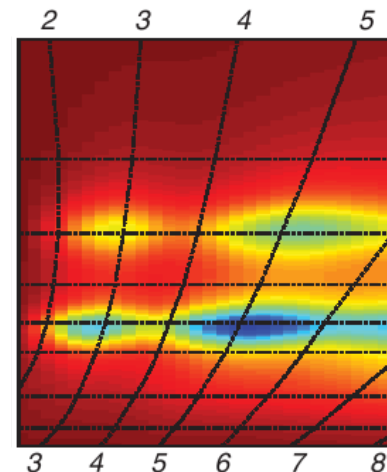
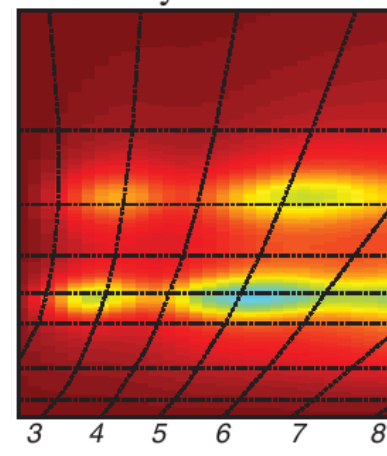
$$\Gamma = 1.69(5) \text{ meV}$$

$$d_{\text{Sb-Sb}} = 2.754(15) \text{ \AA}$$

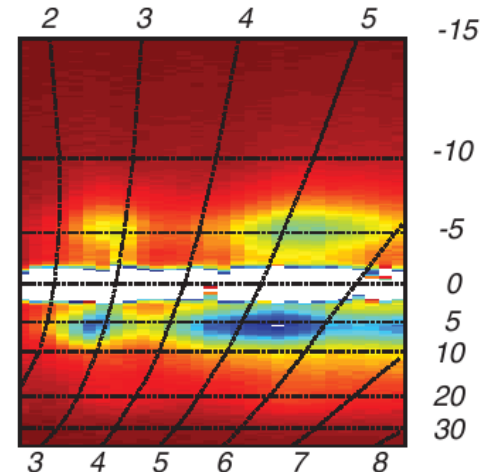
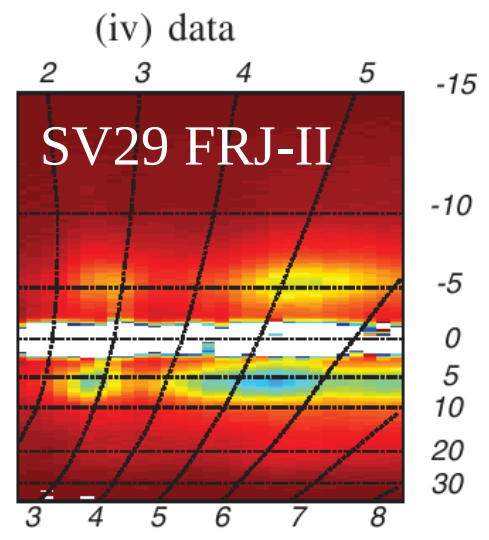
$$u^2_{33} = 0.04 \text{ \AA}$$



(iii) longitudinal
weakly correlated



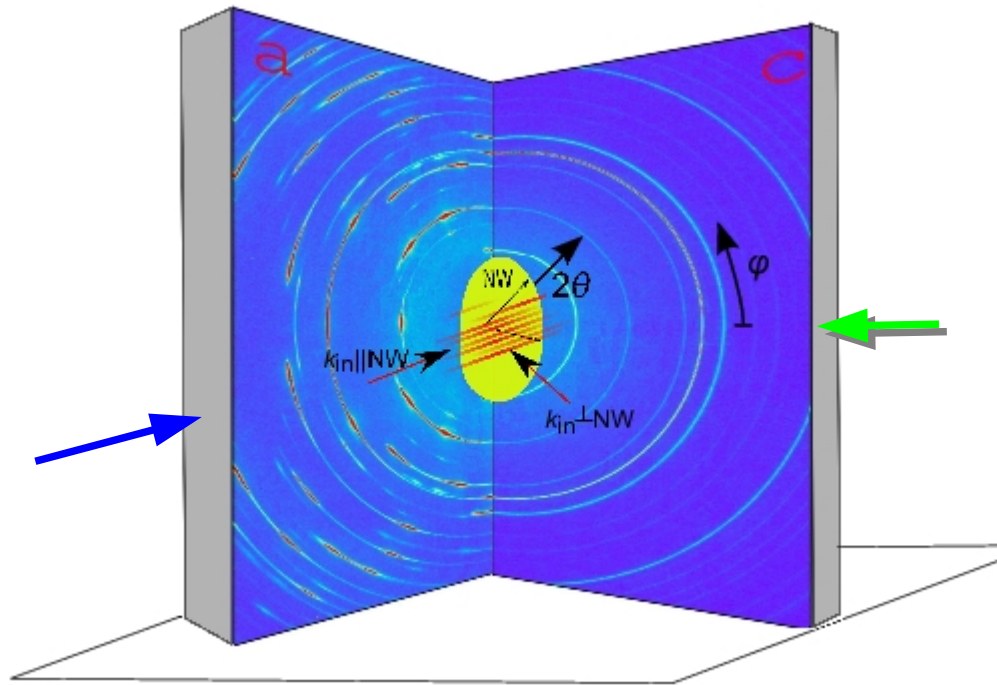
$Q (\text{\AA}^{-1})$



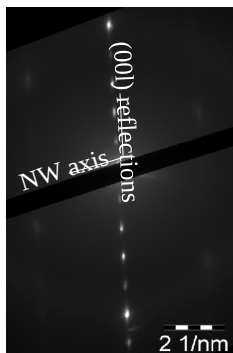
$Q (\text{\AA}^{-1})$

SV29 FRJ-II

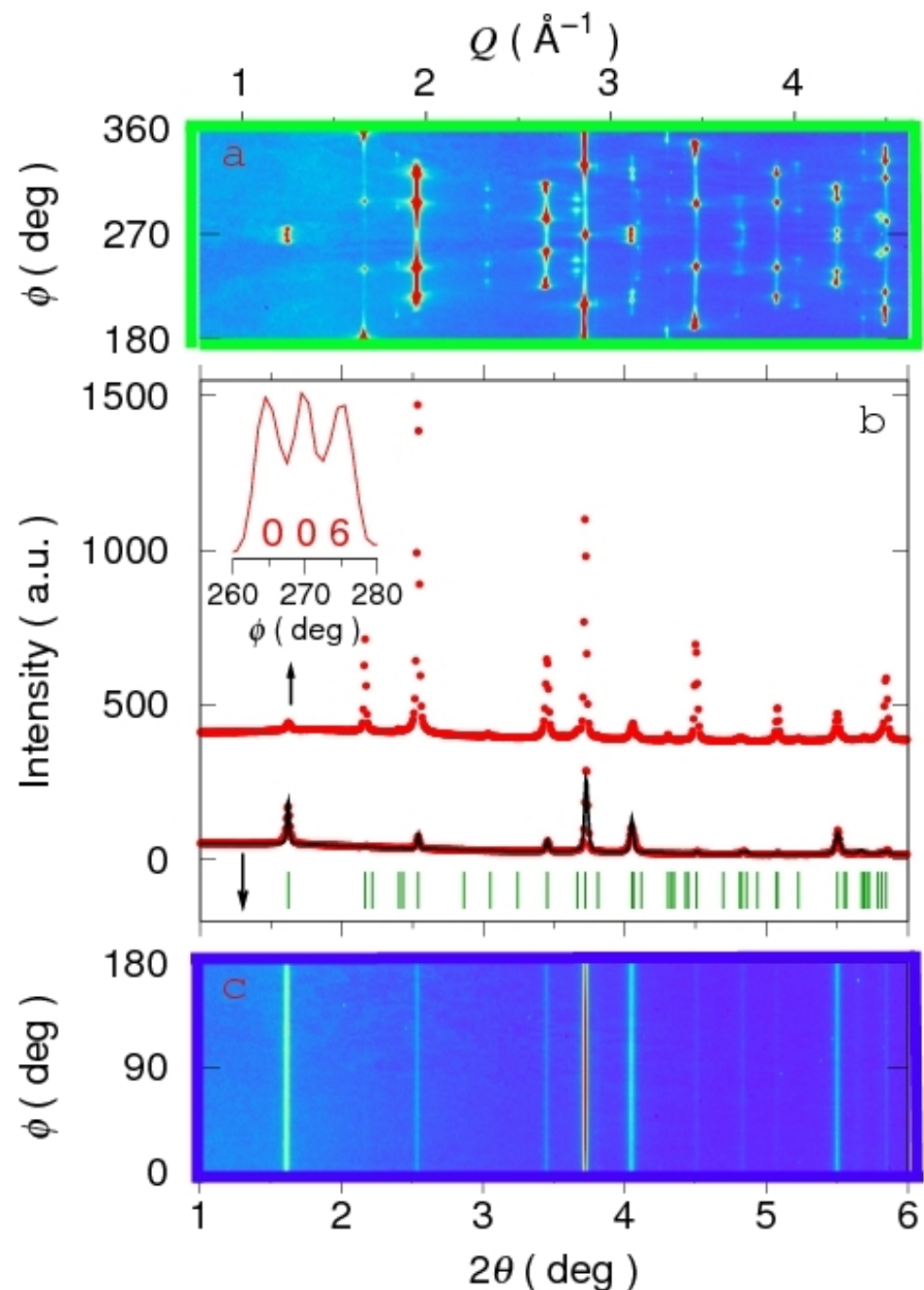
$\text{Bi}_2^{125}\text{Te}_3$ nanowires Ø55 nm



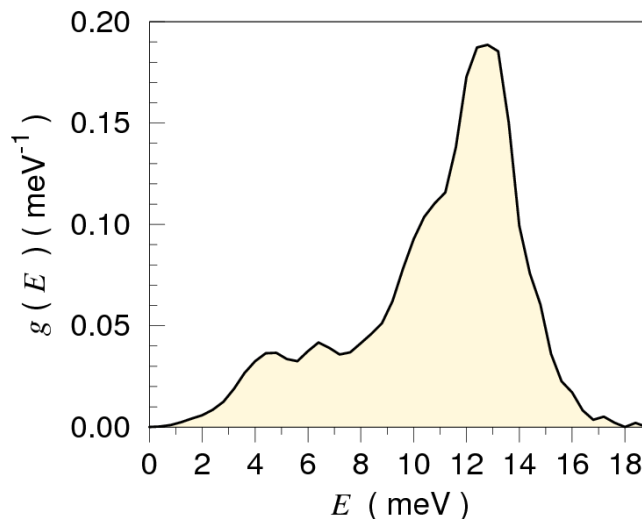
- NW are single crystalline with (0 0 1) twin boundaries
- Larger diameter NW are highly textured
- c-axis at 85 deg w/r to NW axis



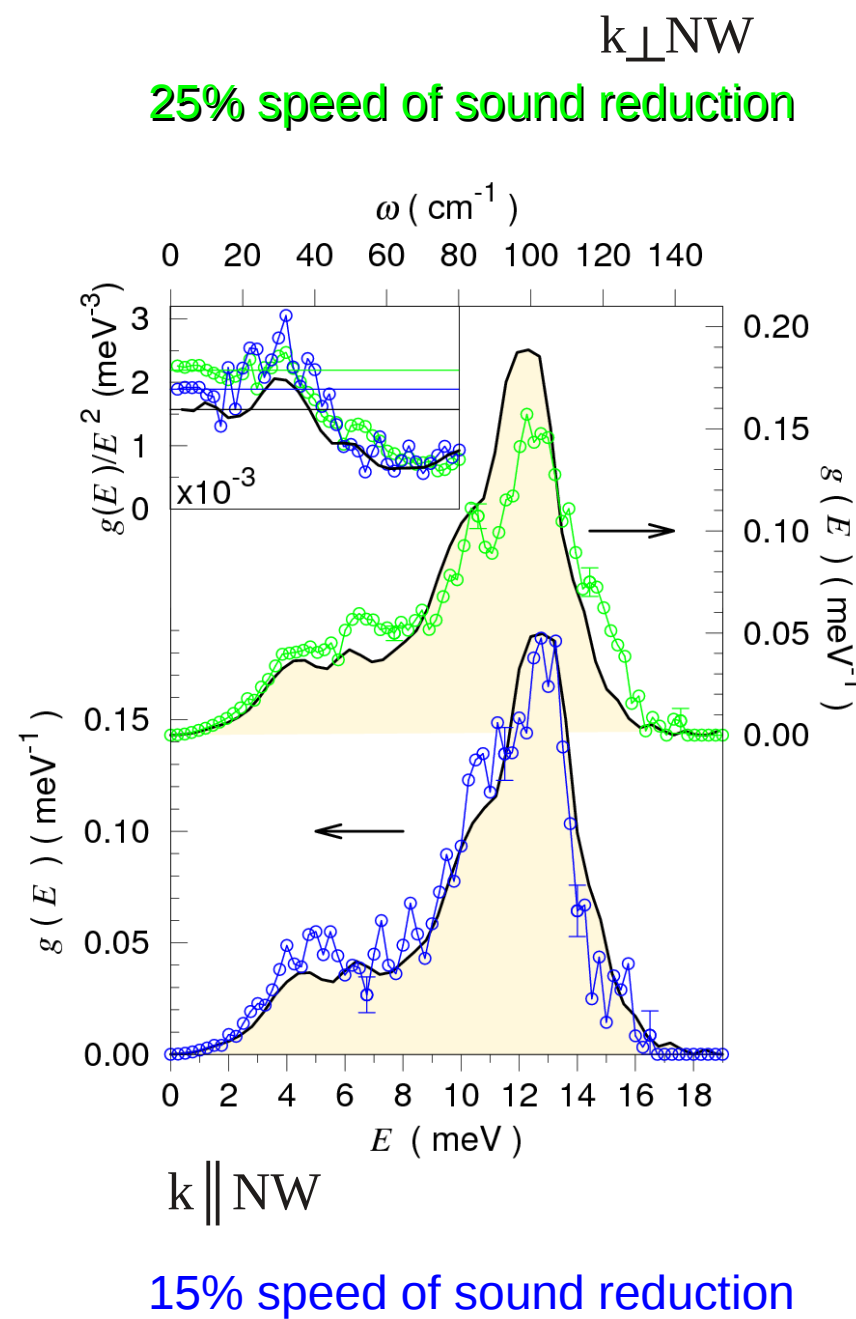
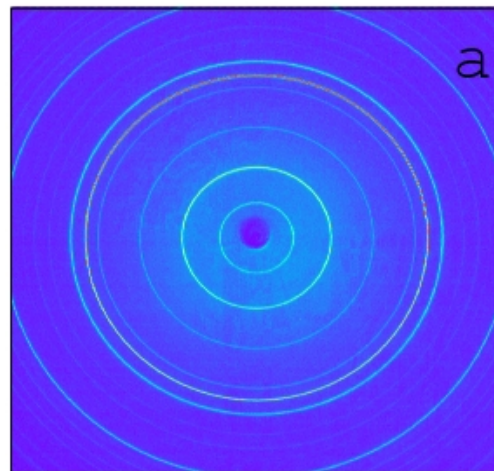
Z. Aabdin, U. Tübingen



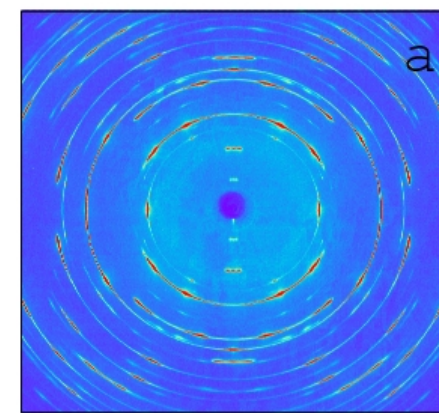
$\text{Bi}_2^{125}\text{Te}_3$ nanowires Ø55 nm: ^{125}Te phonons



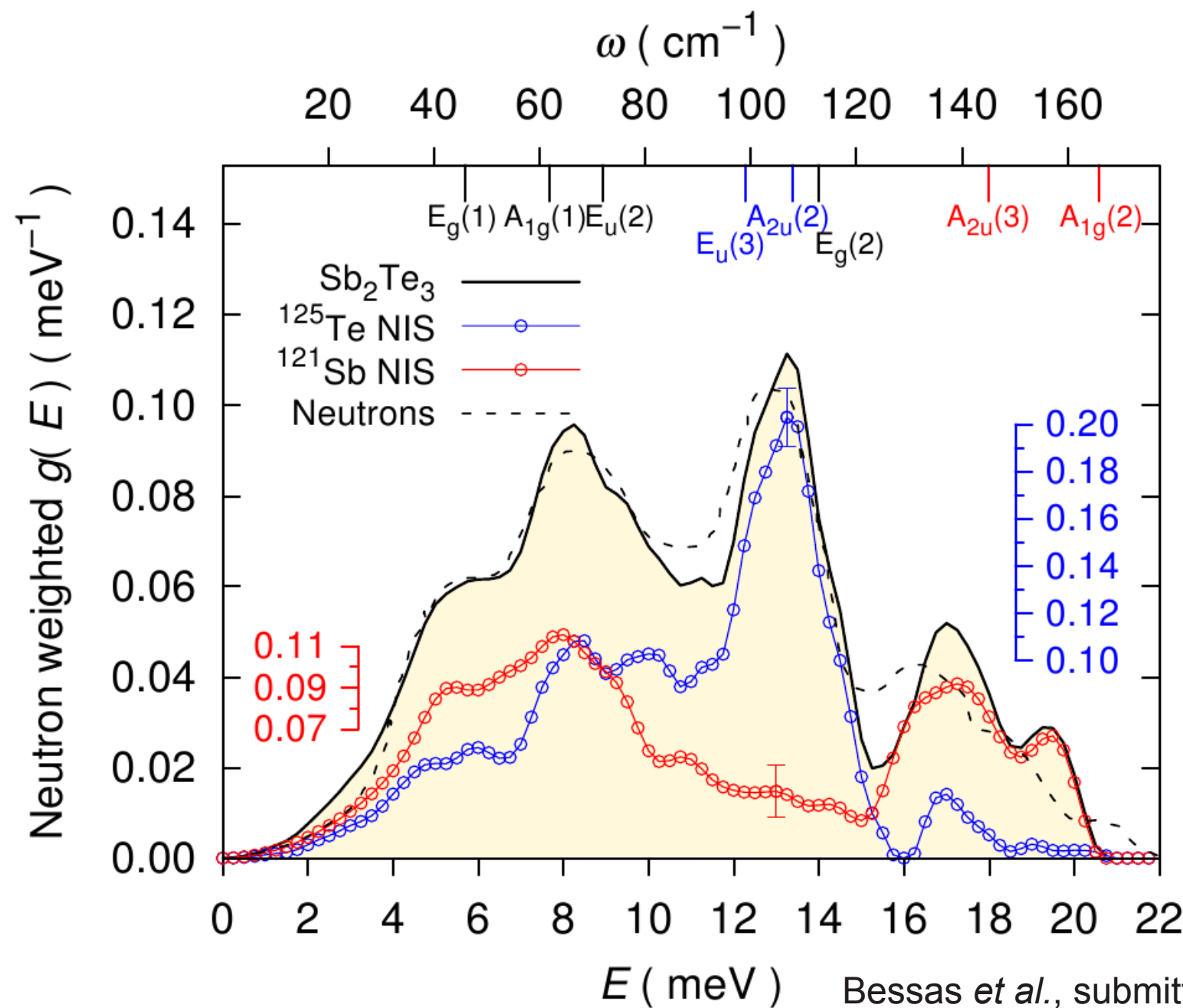
Bulk: $v_s = 1750$ km/s



25% speed of sound reduction

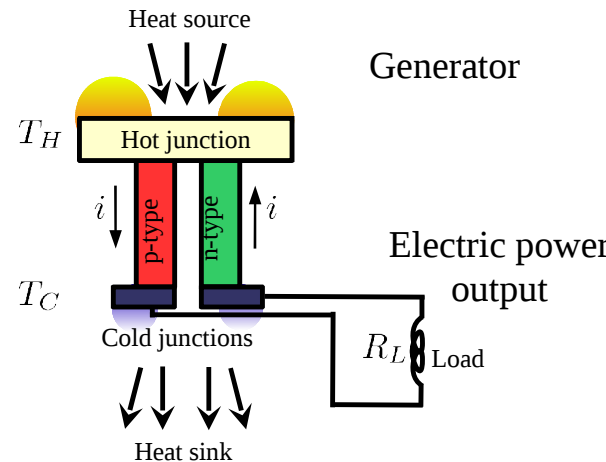


Density of phonon states – Bulk Sb_2Te_3



Generator efficiency

$$\eta = \left| \frac{P}{\dot{Q}} \right| = \left| \frac{R_L I^2}{\dot{Q}} \right|$$



Peltier heat loss ($\pi I < 0$) Joule heat gain Thermal conductivity loss

$$\dot{Q} = -\pi_{ab}I - \frac{I^2}{2}[\rho_a + \frac{\rho_b}{B}]L + (\kappa_a + B\kappa_b)\Delta T/L$$

Optimization for maximal efficiency yields

$$\eta = \eta_C \frac{\sqrt{1 + Z_{ab}T_{av}} - 1}{\sqrt{1 + Z_{ab}T_{av}} + T_C/T_H}$$

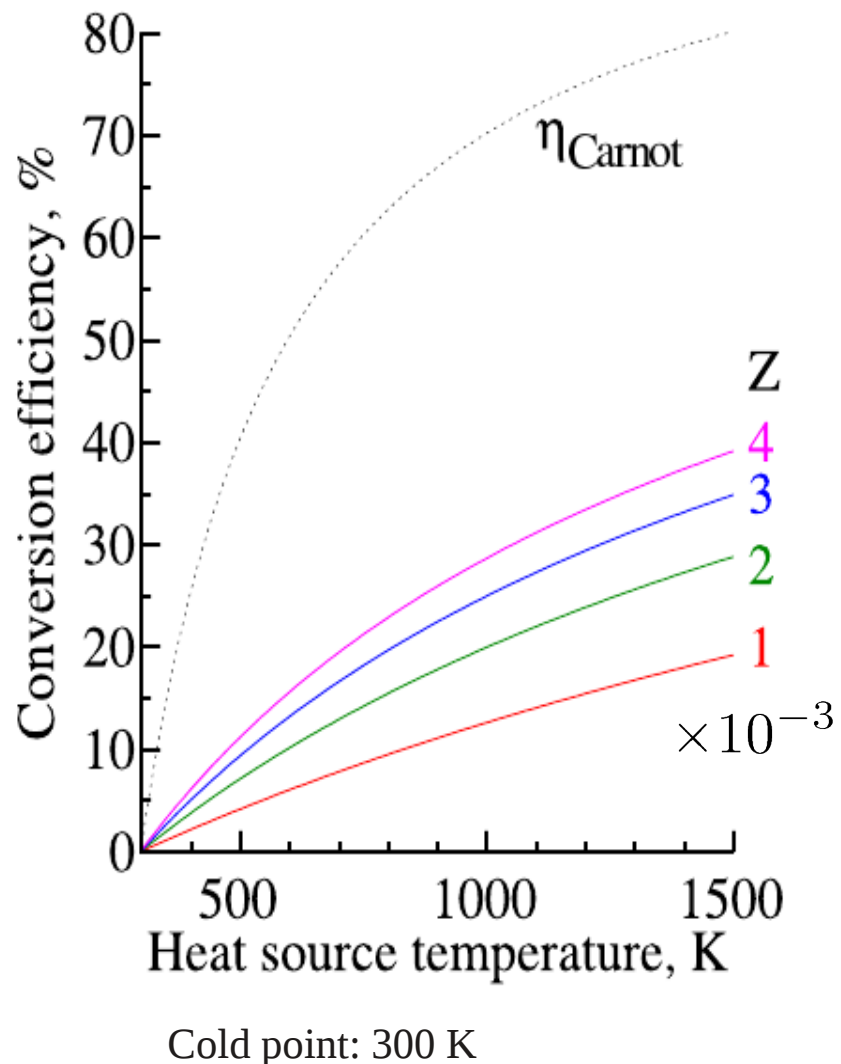
with

$$Z_{ab} = \alpha_{ab}^2 / [(\rho_a \kappa_a)^{1/2} + (\rho_b \kappa_b)^{1/2}]^2$$

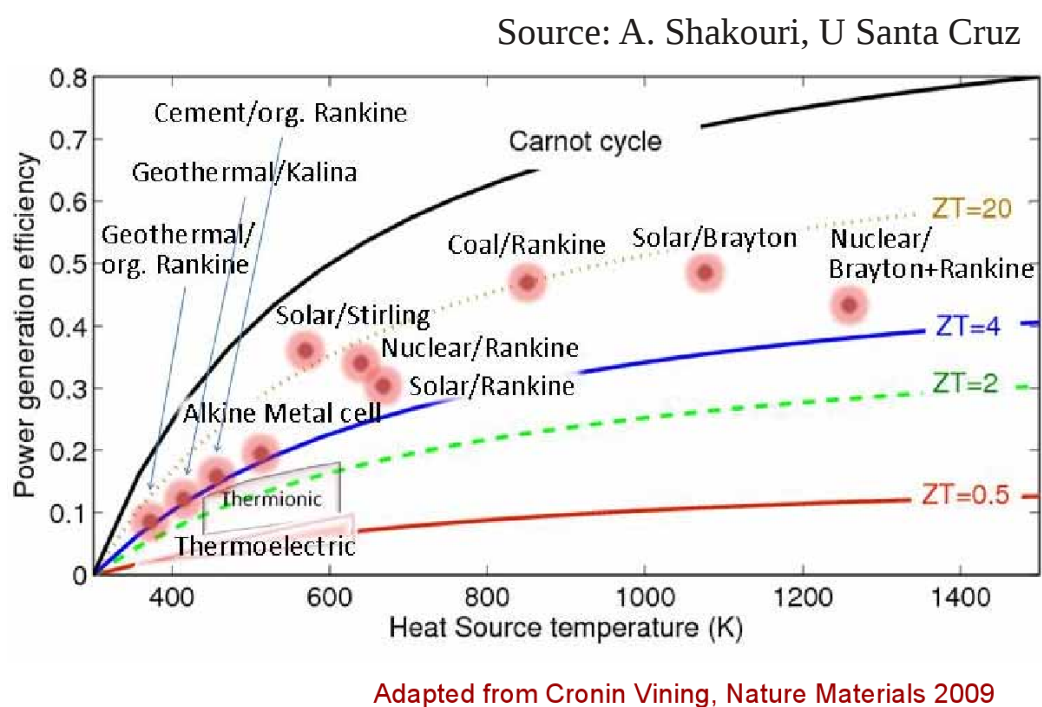
Considering a single material

$$Z = \frac{\alpha^2}{\rho\kappa} = \frac{\alpha^2\sigma}{\kappa}$$

Generator conversion efficiency

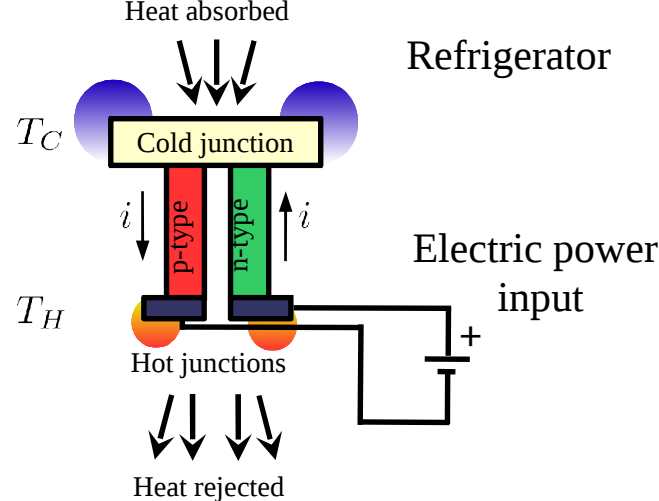


$$Z = \frac{\alpha^2 \sigma}{\kappa} \rightarrow \text{Power factor}$$



NB: Z is the figure of merit [1/K], ZT is the dimensionless figure of merit.

Refrigerator efficiency



$$COP = \left| \frac{\dot{Q}}{P} \right| = \left| \frac{\dot{Q}}{VI} \right|$$

$$P = RI^2 + \alpha_{ab}\Delta TI$$

Peltier cooling

Joule heating

Thermal conductivity

$$\dot{Q} = \alpha_{ab}T_C I - \frac{I^2}{2}R - (\kappa_a + B\kappa_b)\Delta T/L$$

$$R = [\rho_a + \frac{\rho_b}{B}]L$$

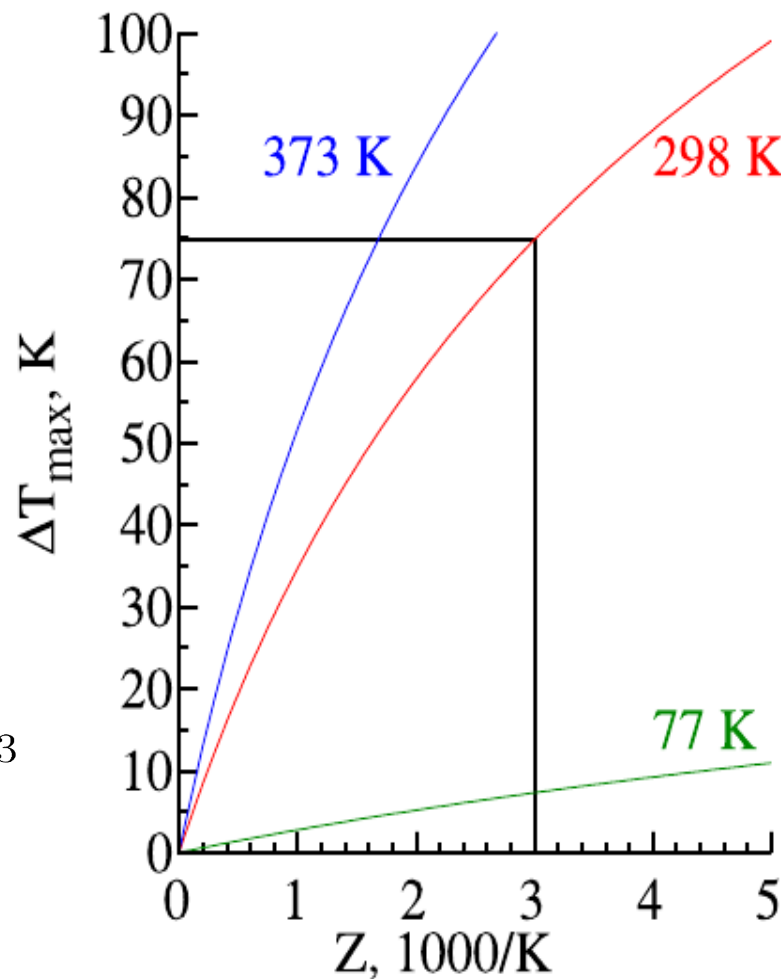
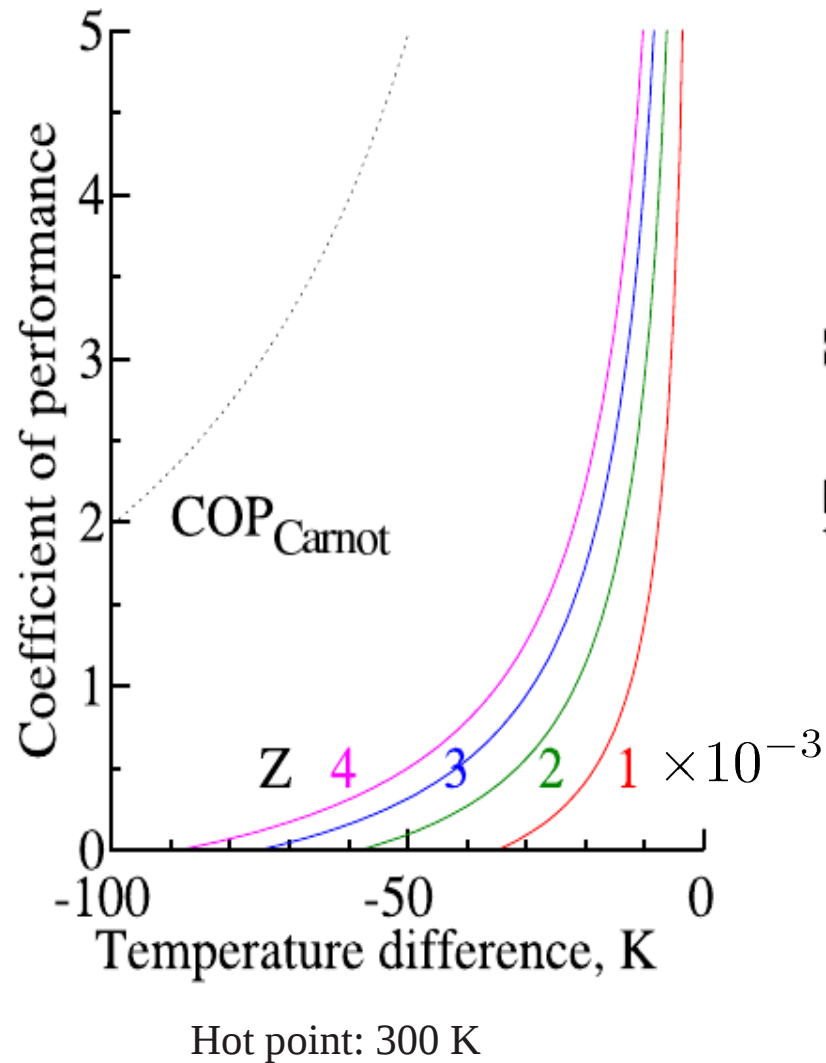
Optimization for maximal cooling power yields

$$\Delta T = ZT_C^2/2 \quad I_o = \alpha_{ab}T_C/R$$

Optimization for maximal efficiency yields

$$COP = \frac{T_C}{T_H - T_C} \frac{\sqrt{1 + Z_{ab}T_{av}} - T_H/T_C}{\sqrt{1 + Z_{ab}T_{av}} + 1}$$

Refrigerator conversion efficiency



Material efficiency

$$Z = \frac{\alpha^2 \sigma}{\kappa} \rightarrow \text{Power factor}$$

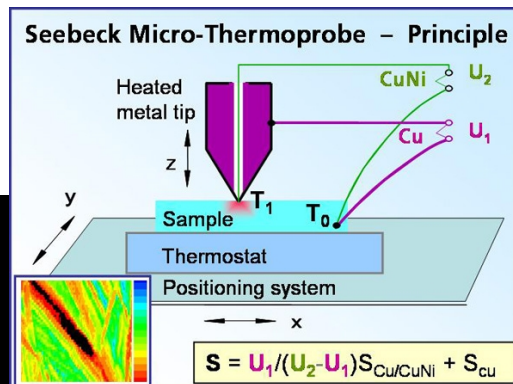
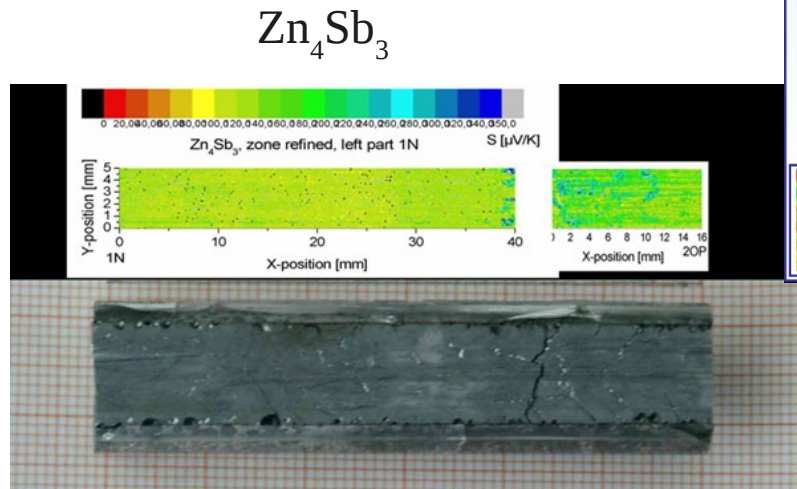
$$\alpha^2 = (\alpha_b - \alpha_a)^2$$

Opposite sign of the thermopower in both legs.

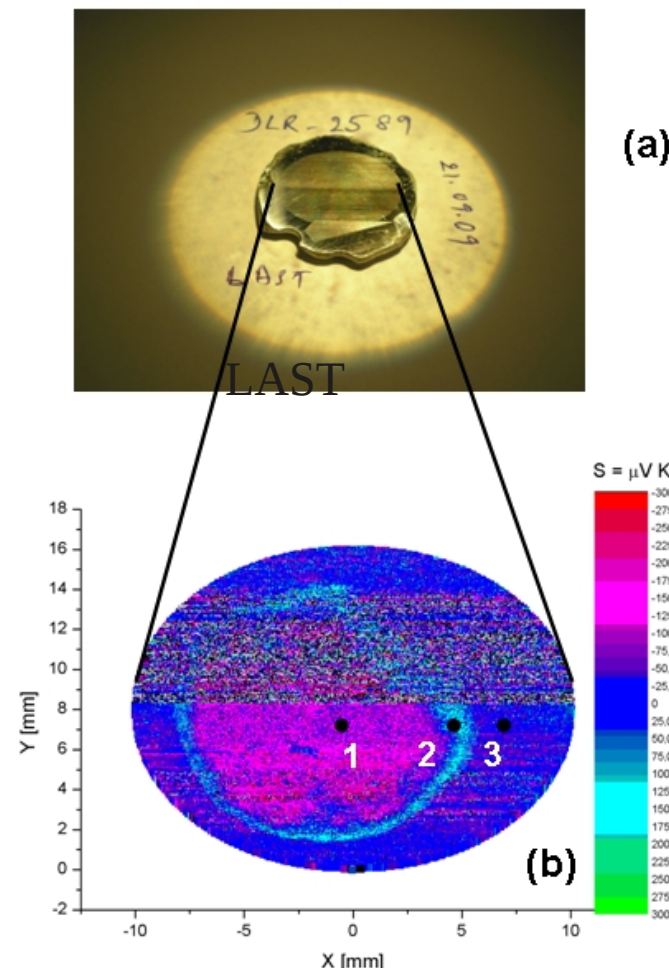
$$\alpha_{n+p} = \frac{\alpha_n \sigma_n + \alpha_p \sigma_p}{\sigma_n + \sigma_p}$$

Avoid bipolar conductivity

In as cast materials, inhomogeneities are observed.



Source: DLR



Typical values and requirements

Goal: $ZT = \frac{\alpha^2 \sigma}{\kappa} T = 1$

Suppose: $\kappa_l = 0$

$$\kappa_e / \sigma \approx L \cdot T \Rightarrow ZT = \frac{\alpha^2 \sigma}{\kappa_e} T = \alpha^2 / L = 1$$
$$\alpha = \sqrt{L} = 157 \mu\text{V/K}$$

Compare with Sommerfeld model for the free electron gas

$$\alpha \sim -c_v / 3ne \quad \alpha = -142(k_B T / E_F) \mu\text{V/K}$$

$$c_v = \pi^2 / 3k_B^2 T g(E_F) \quad E_F \sim 10000 \text{ K}$$

Slack „limit“ for the minimal thermal conductivity in bulk crystalline materials

$$\kappa_{min} \simeq 0.25 - 0.5 \text{ Wm}^{-1}\text{K}^{-1}$$

$$\kappa_{air} \simeq 0.024 \text{ Wm}^{-1}\text{K}^{-1}$$

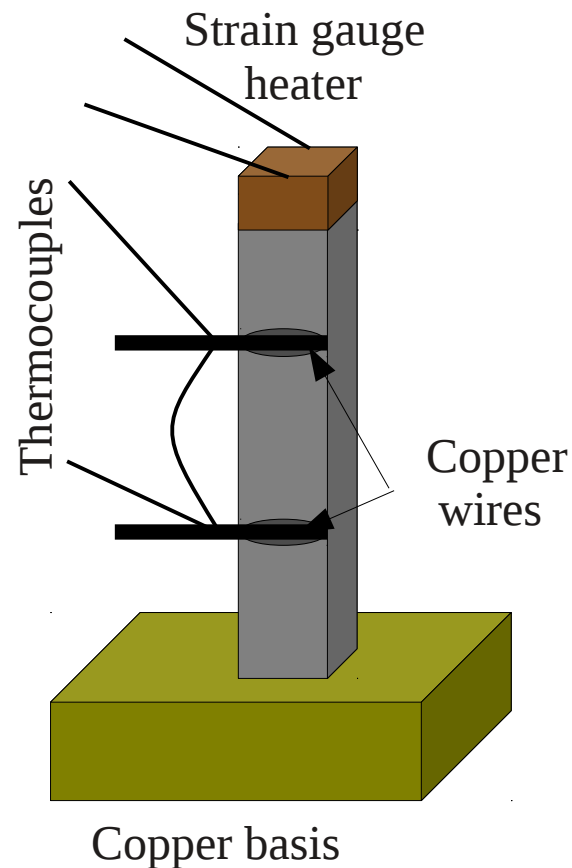
Characterization

$$Z = \frac{\alpha^2 \sigma}{\kappa}$$

Complex problem:

- 3 quantities must be measured
- Error bars are often large on ZT
- High temperature measurements are challenging
(radiative losses, corrosion, ...)

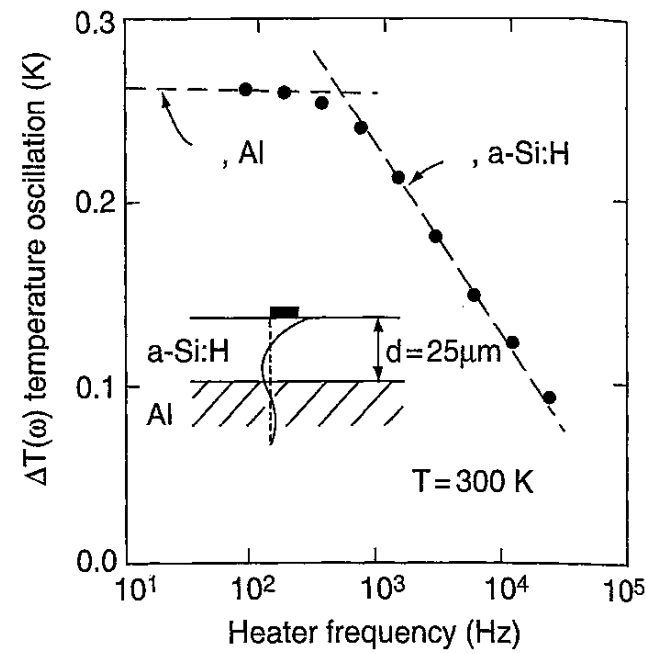
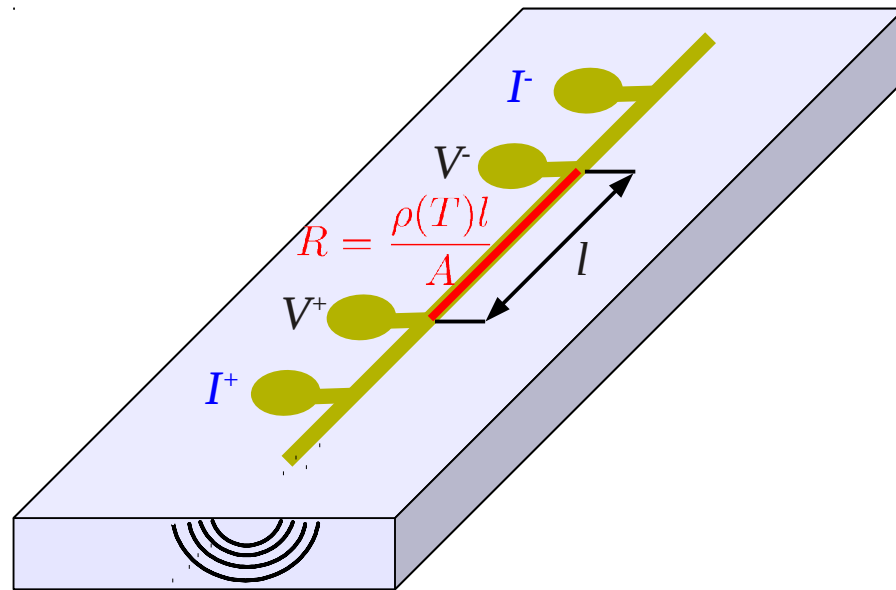
Four point thermal conductivity
and Seebeck measurements



Characterization

AC thermal transport: „3ω“ method

$$V = IR = I_0 e^{i\omega t} \left(R_0 + \frac{dR}{dT} \Delta T \right) = V_1 e^{i\omega t} + V_3 e^{i3\omega t}$$



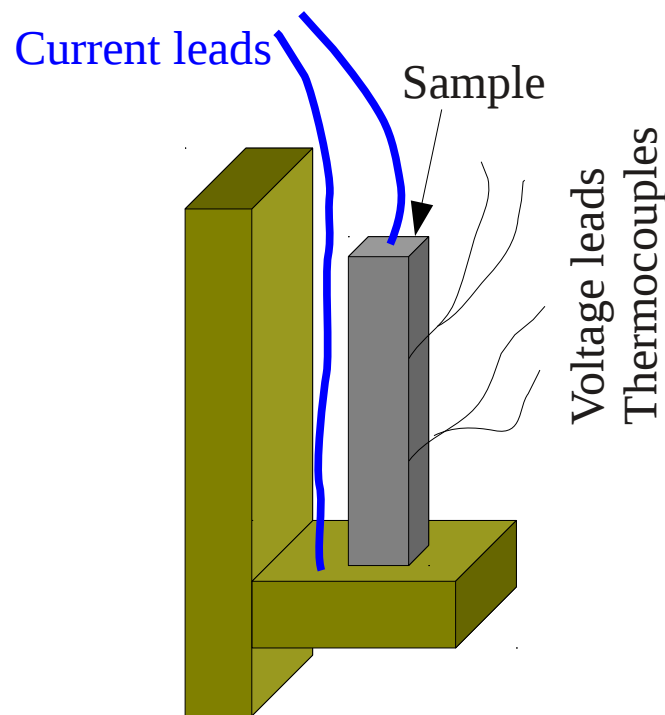
$$\kappa = \frac{V_1^3(\omega) \ln(\omega_1/\omega_2)}{4\pi l R^2 [V_3(\omega_2) - V_3(\omega_1)]} \frac{dR}{dT}$$

Applicable for films

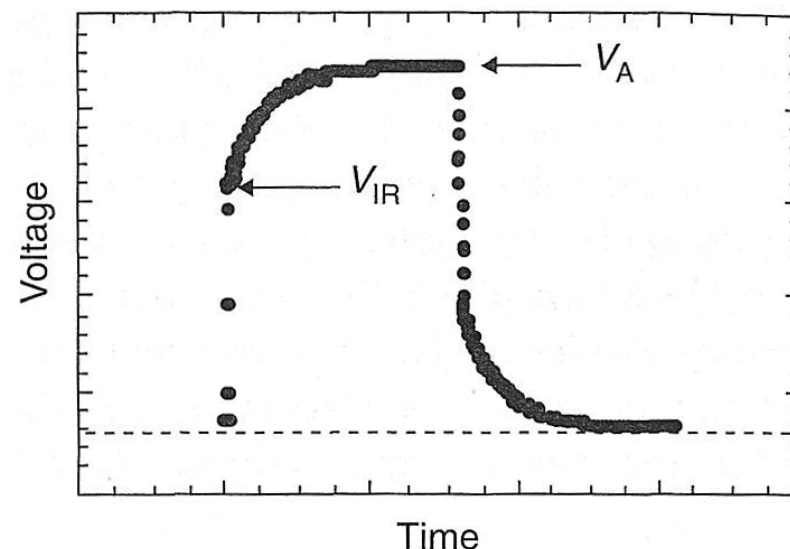
Characterization

Z-Meter - Harman method

Measures the „device Z“, but requires high-Z materials



$$V_A = V_R + V_{TE}$$



$$ZT = \left(\frac{V_A}{V_{IR}} - 1 \right)$$